



VCU

Virginia Commonwealth University
VCU Scholars Compass

Theses and Dissertations

Graduate School

2013

REGULATION OF SATIETY QUIESCENCE: CYCLIC GMP, TGF BETA, AND THE ASI NEURON

Thomas Gallagher
Virginia Commonwealth University

Follow this and additional works at: <https://scholarscompass.vcu.edu/etd>



Part of the [Biochemistry, Biophysics, and Structural Biology Commons](#)

© The Author

Downloaded from

<https://scholarscompass.vcu.edu/etd/3254>

This Dissertation is brought to you for free and open access by the Graduate School at VCU Scholars Compass. It has been accepted for inclusion in Theses and Dissertations by an authorized administrator of VCU Scholars Compass. For more information, please contact libcompass@vcu.edu.

© Thomas L. Gallagher, 2013

All Rights Reserved

REGULATION OF SATIETY QUIESCENCE:
CYCLIC GMP, TGF BETA, AND THE ASI NEURON

A dissertation submitted in partial fulfillment of the requirements for the degree
of Doctor of Philosophy at Virginia Commonwealth University.

by

THOMAS L. GALLAGHER

Bachelors of Science, State University of New York College at Geneseo, 2008

Director: Young-jai You, Ph.D.

Department of Biochemistry and Molecular Biology

Virginia Commonwealth University

Richmond, Virginia

December 2013

Acknowledgement

I would like to express my deepest gratitude to Young You and Leon Avery for their time and effort in teaching me what it is to be a scientist and providing me the opportunity to train in becoming one.

I would also like to thank my committee members Drs. Jill Bettinger, Andrew Davies, Andrew Larner, and Keith Baker for their input, feedback, and tough questions that helped improve this project every step of the way. Further, I am very grateful to Drs. Bettinger and Davies who allowed me to begin this project using equipment and software in their lab without which this project would still be in its infancy.

I am deeply grateful to my friends and family for the support they have given me this point in my life. I would especially like to thank my wife, Allison Dupler, for her love and encouragement through these past several years.

Table of Contents

	Page
Acknowledgements.....	iii
List of Figures.....	v
Chapter	
1 Background.....	12
1.1 The epidemic of obesity.....	12
1.2 Satiety.....	13
1.3 <i>Caenorhabditis elegans</i> as a model system.....	15
1.4 Worm behavior and behavioral states.....	16
1.5 TGF β and cGMP signaling in satiety quiescence.....	18
2 Results and Discussion.....	22
2.1 Roaming, dwelling, and quiescence can be detected by HMM analysis- Motion recording and analysis.....	22
2.2 Unbiased state discovery.....	38
2.3 Are there discrete locomotive behavioral states?.....	43
2.4 Behavioral states are arranged in a triangle.....	45
2.5 Verifying previous results with TOBO.....	50
2.6 TGF β regulation of satiety quiescence.....	55
2.7 <i>egl-4</i> signaling in satiety quiescence.....	64

2.8 ASI is activated by nutrition.....	67
2.9 Additional satiety signaling.....	73
3 Conclusions and Future Directions.....	90
4 Materials and Methods.....	96
Literature Cited.....	109

List of Figures

	Page
Figure 1: Worm locomotion reflects nutritional status	23
Figure 2: Treating bacteria with aztreonam increases bacterium size.	26
Figure 3: Motion characteristics of roaming, dwelling, and quiescence	28
Figure 4: Speed histograms, speed, and direction change for roaming, dwelling, and quiescent worms.....	31
Figure 5: Hidden Markov Model analysis, standard state fits.	33
Figure 6: Geometry of behavioral states.	40
Figure 7: Hierarchical cluster analysis of states.	46
Figure 8: Behavioral states are arranged in a triangle.....	48
Figure 9: Locomotion tracking and HMM analysis of repeats satiety quiescence findings	51
Figure 10: TOBO	53
Figure 11: Aztreonam treated bacteria acts as poor quality food	56
Figure 12: TGF β in ASI neurons promote the switch from dwelling to quiescence.....	59
Figure 13: Food and cGMP increase level of DAF-7 in fasted worms	62
Figure 14: Restoring egl-4 expression rescues satiety quiescence	65
Figure 15: EGL-4 function for quiescence	69

Figure 16: <i>egl-4</i> worms respond to nutritional state and food quality.....	71
Figure 17: ASI responds to nutrition	74
Figure 18: CB1 receptor inhibitor treatment increases roaming behavior.....	77
Figure 19: Endocannabinoid signaling regulation of satiety quiescence.....	79
Figure 20: Worms with feeding defects show altered quiescence behavior.	81
Figure 21: Selected neuropeptide mutants show no change in quiescence	84
Figure 22: Multidrug resistance protein genes may play a role in conveying satiety signals.	86
Figure 23: <i>glr-1</i> has no effect on quiescence.....	88
Figure 24: Proposed model of satiety quiescence signaling of cGMP and TGF β in ASI \rightarrow RIM + RIC.....	93
Figure 25: HMM fit scheme.	100

List of Abbreviations

cGMP	cyclic Guanosine Monophosphate
GFP	Green Fluorescent Protein
HMM	Hidden Markov Model
MRP	Multidrug Resistant Protein
NAE	N-acylethanolamine
NGM	Nematode Growth Medium
TGF β	Transforming Growth Factor beta

Abstract

Regulation of Satiety Quiescence: cyclic GMP, TGF beta, and the ASI Neuron

By Thomas L. Gallagher

A Dissertation submitted in partial fulfillment of the requirements for the degree of
Doctor of Philosophy at Virginia Commonwealth University.

Virginia Commonwealth University, 2013

Major Director: Young-Jai You, Ph.D.

Assistant Professor, Department of Biochemistry and Molecular Biology

The worm *Caenorhabditis elegans* is a well-studied model organism in numerous aspects of its biology. This small free living nematode has less than 1,000 cells, but shows clear conservation in both signaling and behavior to mammals in aspects of appetite control. This is of importance to humans, where failure of appetite control is a major factor in the unprecedented obesity epidemic that we see today.

In general, worm behavior reflects its internal nutritional state and the availability and quality of food. Specifically, worms show a behavioral state that mimics aspects of the mammalian behavioral satiety sequence, which has been termed satiety quiescence. We have used locomotion tracking and Hidden Markov Model analysis to identify worm behavioral state over time, finding quiescence along with the established worm locomotive behaviors roaming and dwelling. Using this analysis as well as more conventional cell biology and genetic approaches we have further investigated satiety signaling pathways. We have found that the neuron ASI is a major center of integration of signals regarding the internal nutritional state of the worms as well as the nutritional content of its environment. Our results show that cGMP causes levels of the TGF β ligand to be increased in fasted worms, which is then released and binds to its receptor on the RIM and RIC neurons. This signaling connects nutritional state to behavioral response, promoting the sleep-like behavioral state satiety quiescence. Additionally, we have begun a candidate approach examining several other groups of signaling molecules for potential roles in satiety quiescence signaling including cannabinoids, multidrug resistance proteins, and neuropeptides. The result of this investigation is a better understanding of mechanisms of

satiety quiescence signaling as well as a new tool that provides highly quantitative, unbiased, and automated data to aid in our ongoing work.

Clarification of Contributions

The experiments which generated the data for all figures in this document were conducted by Thomas Gallagher. Experiments were designed by Thomas Gallagher, Dr. Young-Jai You, and Dr. Leon Avery. Locomotion tracking experiments done on the multi-camera platform (frame built by former Avery lab member Dr. Boris Shtonda) were analyzed using software written by Thomas Gallagher. The Hidden Markov model analysis software was written by Leon Avery. Calcium imaging experiments were conducted in the lab of Dr. Rex Kerr at Howard Hughes Medical Institute at Janelia Farms. Calcium imaging data was analyzed blind by Rex Kerr using custom written software. Worm strains were kindly provided by Drs. Kaveh Ashrafi, Mark Alkema, Matthew Beverly, Piali Sengupta, Matthew Gill, Annette McGehee as well as the Caenorhabditis Genetics Center. Numerous transgenic strains used were constructed by Dr. Jeongho Kim. Microfluidic devices used for calcium imaging were kindly provided by Dr. Manuel Zimmer. This work was supported by the Virginia Commonwealth University Department of Biochemistry and Molecular Biology as well as National Institutes of Health and American Heart Association grants to Young-Jai You and Leon Avery.

Regulation of Satiety Quiescence: cyclic GMP, TGF beta, and the ASI Neuron

*Portions of this work appear in the publications ‘The Geometry of Locomotive Behavioral States in *C. elegans*’ Gallagher et al. (2013) PLOS ONE and ‘ASI Regulates Satiety’ Gallagher et al. (2013) The Journal of Neuroscience.

1. Background

1.1 The Epidemic of Obesity

Energy homeostasis, the balance between food intake and metabolic activity, is an essential function for any organism. Through selective pressure, animals have adapted mechanisms to survive in times of food surplus and scarcity. In our current environment, we no longer find ourselves in a dynamic state of energy supply and demand; food is constantly available and our lifestyle has become increasingly sedentary, which has led to an epidemic of obesity with one third of the United States population diagnosed as clinically obese (1,2). Obesity leads to numerous secondary health problems including heart disease, diabetes, high blood pressure, liver disease, and cancer, reducing quality of life as well as placing a significant burden on the healthcare system (3). Understanding of the causes of obesity will allow for new and more effective approaches to treat the underlying problem of obesity rather than the secondary health conditions that arise from it.

While obesity is a result of complex interactions among biology, behavior, and environment, twin, adoption, and other family studies show that there is a heritable component to body mass index (4). Observing obesity trends in the United States suggests that there is a subset of our population that is susceptible to obesity and a subset that is resistant to obesity (4–6). Since the discovery of the leptin gene and its receptor (7,8), investigation of “obesity genes” has opened the research into molecular components of obesity. These genes are molecular components of the physiological system that regulates energy balance matching energy intake to energy expenditure (8). Currently there are 11

genes known to be monogenic causes of obesity (9). Many of these genes are implicated in appetite control, as the loss of function results in excessive energy intake (10). However, single gene mutation accounts for only 5-6% of severe cases of childhood obesity (5).

Much more relevant to the widespread problem of obesity is the complex signaling which regulates the balance of energy intake, storage, mobilization, and expenditure. These genes encode the physiological components of energy regulation where single nucleotide polymorphisms and regulation at the transcriptional, translational, and post-translational levels are likely to lead to predisposition or resistance to obesity. It is desirable to have a complete understanding of the molecular mechanisms of energy metabolism. One of the most significant factors in energy imbalance is the mechanism of appetite control.

1.2 Satiety

Satiety, the sensation of being full that causes the cessation of feeding, is governed in mammals by a complex signaling pathway that originates in the gut, is conveyed by several endocrine signaling pathways, and is integrated in the central nervous system (11,12). This signaling has been found to result in a fixed behavioral sequence where the animal stops eating, grooms itself and explores for a short time, then rests or sleeps in what has been termed the Behavioral Satiety Sequence (13–15). This behavior is widely conserved, having also been observed in birds (16). In mammals, satiety signals from the gut and adiposity-related signals are communicated by endocrine factors which are integrated in the hypothalamus (11,12,17). The hypothalamus has been well established as

a site of appetite control regulation, starting with classical experiments by Hetherington and Ranson (1940) where food intake could be increased to induce obesity or decreased to induce starvation depending on which area of the hypothalamus was damaged by electrolytic lesions (18,19). This points to a major component of appetite control regulation being signaled neuronally.

Recently, our lab has found a behavior in *C. elegans* that resembles mammalian satiety. After being fasted and refed, worms stop moving, stop feeding, and enter a sleep-like state termed satiety quiescence (20). Like mammalian satiety, satiety quiescence depends requires high quality food and originates with signals from the gut, and is conveyed by neuropeptides (20).

Satiety quiescence behavior is regulated by insulin, Transforming Growth Factor beta (TGF β), and cyclic Guanosine Monophosphate (cGMP). Insulin is well known to control food intake in mammals and TGF β has been linked to the anorexia seen in cancer patients (21,22). Recently, Valentino et al. (23) showed that mice lacking the uroguanylin gene, which encodes a ligand for a membrane bound guanylate cyclase that produces cGMP, have higher food intake and become obese. They found that the uroguanylin-GUCY2C receptor works as a canonical satiety signaling system: uroguanylin is released from the gut and binds to GUCY2C in the hypothalamus. Together, the fact that these three signaling pathways regulate a conserved behavior indicates that there is a strong evolutionary conservation of the control of food intake in animals, meaning that additional genes discovered in worms to regulate this behavior have a high likelihood to have homologs in mammals with conserved functions.

1.3 *Caenorhabditis elegans* as a model organism

Balancing energy demand with a dynamic environment of nutrient availability is a vital task for all organisms. Therefore the mechanisms that underlie the metabolic, physiological, and behavioral processes essential to energy balance are thought to have evolutionarily ancient origins (24,25). The nematode *Caenorhabditis elegans* has recently emerged as a leading model for studying energy metabolism (24,26–28), where many molecules and mechanisms of action are conserved but the signaling pathways and neuronal circuitry are much simpler, making them easier to elucidate than mammalian systems.

C. elegans are self-fertilizing hermaphrodites (~0.05% become males through a non-disjunction event of the sex chromosome), have 959 somatic cells, including 302 neurons, and have an invariant developmental cell lineage. They grow from an egg to a reproductive adult in ~2.5 days, and produce ~300 progeny. They are easily and cheaply cultivated in large numbers in lab conditions. Importantly, they are very genetically malleable, with transgenic animals created simply by injecting a transgene into the gonad of an adult, and RNA interference accomplished simply by feeding RNAi expressing bacteria to the worms. Combined with the ease of cultivating animals in large numbers, worms are an attractive model organism for forward and reverse genetic screens to uncover new signaling components in a variety of pathways. This has made the worms a powerful genetic system and has allowed for genome wide investigation into the numerous aspects of energy metabolism and resulted in the discovery of many new genes playing key roles in a variety of pathways involved in energy metabolism (24,27).

1.4 Worm behavior and behavioral states

Food is one of the most important determinants of an animal's behavior. Some of the effects of food are obvious: if there is food, an animal may eat, while if there is no food, or if the food available is poor in quality, it may instead search for new food (see, e.g., Shtonda and Avery (29)). But other effects are complex and depend on the animal's internal state: how recently it has eaten, the presence of food in the digestive tract, the quantity and nature of stored reserves such as fat or glycogen. Information about nutritional state is communicated within the animal by a complex and only partly understood system of signals, and much of the animal's computational machinery is devoted to dealing with food and nutrition (30). Better understanding of these signals might help in treating disorders of feeding, nutrition, and energy balance ranging from anorexia to obesity.

C. elegans feed by pumping bacteria through the pharynx into a teeth-like structure called the grinder, which is connected to the intestine (31). Food availability and feeding history are two of the most significant factors affecting worm feeding behavior (32–35). Food seeking behavior in worms is modulated by food quality (which we have operationally defined by the ability of the bacteria to support worm growth), which correlates inversely with bacterial size (29).

Despite its simple nervous system, the nematode *C. elegans* has a complex array of signals to control feeding and food-related behavior (28,36,37). Indeed, it is only a small oversimplification to say that in the *C. elegans* hermaphrodite *all* behavior is food-related, since food and nutritional state affect every behavior that has been tested, often

profoundly. Locomotive behavior has been studied with particular intensity. Previous workers have described three behavioral states that characterize the locomotive response to food: roaming, dwelling, and quiescence.

When actively feeding, worms alternate between roaming and dwelling (38–40). Roaming worms move swiftly and relatively directly from one place to another, while dwelling worms move slowly and reverse frequently, thus covering little distance. Roaming and dwelling are respectively exploration and exploitation behaviors. Shtonda and Avery (29) and Ben Arous et al. (39) showed that worms roam more on low-quality food and dwell more on high-quality food. An additional behavioral state, quiescence, has recently been identified and characterized as a sleep-like state (20,41,42). We found that worms enter quiescence when they become satiated (20). Together, these studies show that locomotive activity is determined by nutritional status and that nutritional status can regulate switching between behavioral states.

Studying satiety quiescence is problematic because quiescent worms are easily disturbed; quiescent worms wake up after about a minute of observation under conditions where they spend most of their time in quiescence (20,43). While locomotion tracking to identify behavioral state has become more common, a consistent method of identifying behavioral states has not emerged (29,38,39,44). These methods of behavioral state identification parse roaming and dwelling but do not lend themselves to identifying quiescence. Additionally, attempts to identify behavioral state have not been done under conditions where satiety quiescence is enhanced- fasting and refeeding worms on high quality food. One consequence of this limitation is that we know little of the kinetics of

quiescence: do worms cycle in and out of quiescence, and if so, at what rate? Which molecular mechanisms and which neurons and circuits regulate it? To address these deficiencies, we tracked worm locomotion over long periods of time under conditions where satiety quiescence is enhanced and developed a Hidden Markov Model analysis to identify worm behavioral state over time. Subsequent to our publication of this method (45,46), HMM analysis was used by another *C. elegans* group to identify worm behavioral state (47). However, like previous efforts, this only identifies roaming and dwelling behavior and so the HMM was optimized to a two-state model.

1.5 TGF β and cGMP signaling in satiety quiescence

cGMP and TGF β are two of the major signals regulating worm growth and development. Mutations in both pathways affect dauer formation, egg laying, fat storage, and body size (38,48–52). In addition, both pathways are required for satiety quiescence signaling, where we have shown that a gain of function allele of the cyclic GMP dependent protein kinase *egl-4* suppresses the quiescence defect of worms with a mutation in the TGF β ligand *daf-7* (20). This places *egl-4* downstream of *daf-7* in satiety quiescence signaling.

cGMP is a potent signaling molecule that is used across diverse taxa from bacteria to humans (53–55). cGMP is synthesized by guanylyl cyclases and degraded by phosphodiesterases, of which worms have 34 guanylyl cyclases (27 receptor type and seven soluble) and four predicted phosphodiesterases (56,57). In worms, guanylyl

cyclases has been shown to play a role in numerous behaviors in addition to satiety quiescence including olfaction, thermosensation, oxygen sensation, and alkalinity sensation (52,58–61).

There are two well-known targets of cGMP in worms: a cyclic GMP dependent kinase, EGL-4, and a cyclic GMP gated channel formed by a heteromeric complex of TAX-2 and TAX-4 (38,62,63). Worms with mutations in these gene show metabolic phenotypes. *tax-2* or *tax-4* mutants show defective chemotaxis, thermotaxis, social feeding, and oxygen sensation and *egl-4* mutants show large body size, increased fat storage, and altered behavior while all mutants have an increased tendency to enter dauer (38,49,62–66). Additionally, there is a gain-of-function allele of *egl-4* in worms that has opposing phenotypes (67).

Importantly, the cGMP-dependent protein kinase has been found to be playing a conserved role in food acquisition and energy homeostasis (68). A natural polymorphism in the gene of this cGMP-dependent protein kinase in *Drosophila* gives rise to two different phenotypes in food seeking behavior and acquisition (69,70). In mice, a cGMP signaling axis has recently been found to convey satiety signaling in the hypothalamus (23). Additionally, there is evidence that cGMP is playing a conserved role in olfaction and taste in mammals (71–73) and learning and memory in both *Drosophila* and mammals (74,75).

The canonical TGF β pathway consists of a ligand binding to type I and type II serine/threonine kinase receptors. Ligand binding causes the receptors to assemble into complexes and activate by phosphorylation. This induces a signaling cascade where Smads

and co-Smads are activated by phosphorylation and translocate to the nucleus to regulate gene transcription. Another class of inhibitory Smads act to antagonize this signaling (76). *C. elegans* have strongly conserved TGF β signaling with several ligands, two type I receptors, one type II receptor, and many Smads and co-Smads with clear orthologs to *Drosophila* and mammalian genes (77).

Mutations in the TGF β pathway in *C. elegans* lead to either constitutive dauer formation or defective dauer formation and this phenotype was used to elucidate the pathway by genetic screens and epistatic analysis (78–81). Dauer formation is where worms enter the dauer diapause, life stage where worms stop developing and are able to weather harsh conditions such as high temperature, overcrowding, and low food (82). Laser ablation of the ASI neuron also makes worms become dauer formation constitutive (83,84).

TGF β can be thought of as a signal to convey that the worm is in a good environment. The TGF β ligand *daf-7* is highly expressed when the worm has abundant food and expressed at a much lower level when the worm is starved (50). High *daf-7* expression causes worms to undergo the reproductive life cycle while low levels of *daf-7* cause worms to become dauers.

While *egl-4* is widely expressed in neurons, intestine, hypodermis and muscle, *daf-7* is expressed in only the ASI neuron (38,49–51,85). However, its receptors *daf-1* and *daf-4* are widely expressed (86–88). The expression of *daf-7* is dependent on the membrane guanylate cyclase DAF-11, which is expressed in at least five pairs of amphid neurons,

including ASI (64,89). Together, this points to a major intersection of cGMP and TGF β signaling pathways in the ASI neuron.

2. Results and Discussion

2.1 Roaming, dwelling, and quiescence can be detected by HMM analysis-

Motion recording and analysis

To quantify quiescence over relatively long time periods, we developed an automated procedure to monitor worms. Because quiescence is suppressed by the presence of other worms (20), only a single worm was recorded at a time. To avoid mechanical disturbance, we did not mechanically track the worm, but instead placed it on a small spot of food, which did not move during recording. To test whether worms became quiescent under these conditions, we measured their speed of movement over time. We found long periods of inactivity under conditions where quiescence is enhanced, fasting and full refeeding on high quality food (Figure 1A). Worms that are not fasted, fasted and refed on poor quality food, or *egl-4(lf)* worms fasted and refed on high quality food did not show this inactivity (Figure 1B-D). Additionally, we found that worms in conditions where quiescence is enhanced show a pattern of switching between active and inactive states (Figure 1E). We initially quantified this data by calculating the average speed and the percent of time at which speed was less than $1 \mu\text{m s}^{-1}$. Average speed was lower and time at low speed was greater under conditions that promote quiescence (Figure 1F,G). These results suggest that satiety quiescence occurred under our recording conditions, although probably not at the level previously inferred for completely undisturbed animals (20).

We operationally define food quality by its ability to support worm growth. This is generally inversely proportional to bacterium size meaning that large bacteria are poor

Figure 1

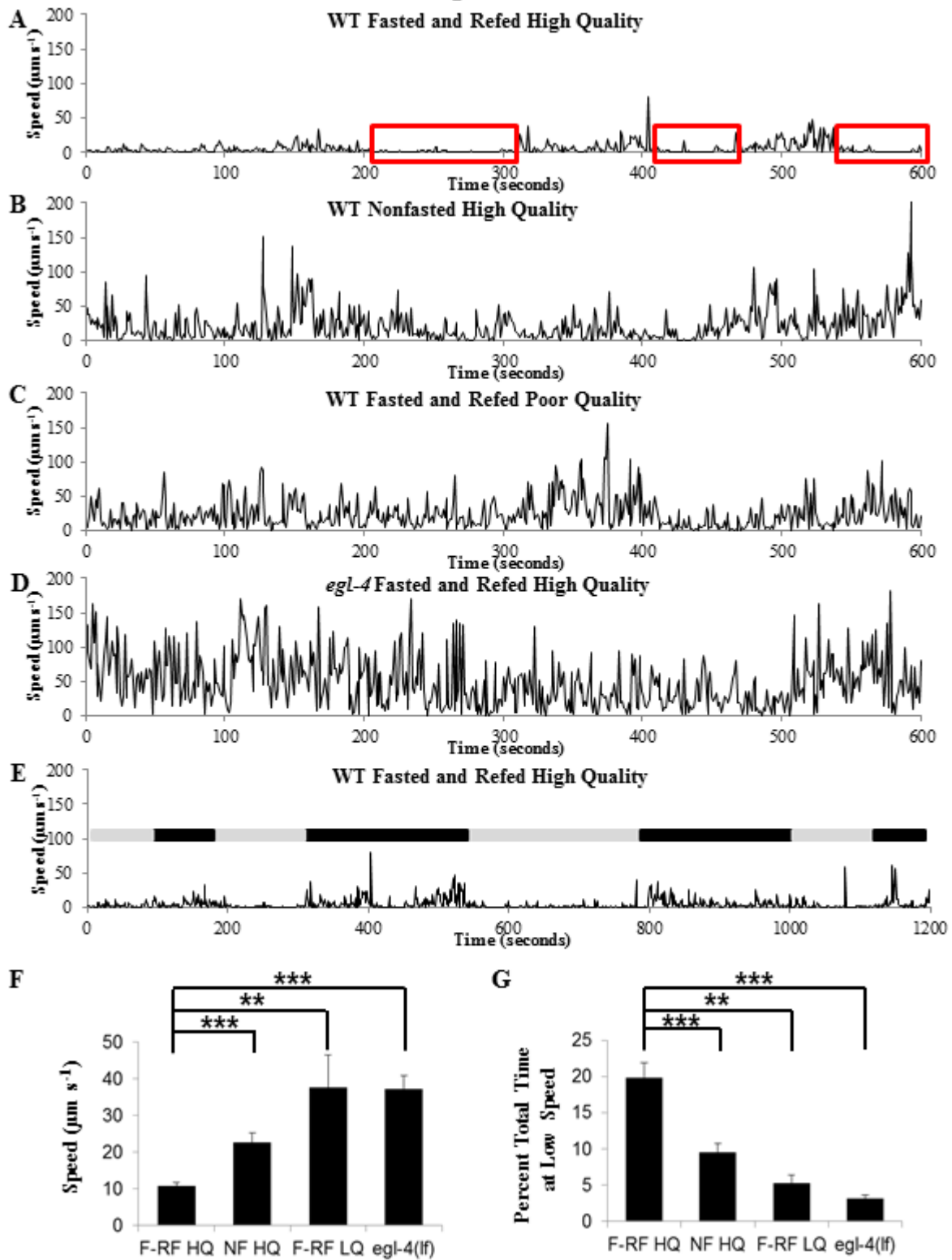


Figure 1. Worm locomotion reflects nutritional status.

A. A representative plot of worm speed over time under conditions where satiety quiescence is enhanced after fasting and refeeding wild-type worms on high quality food.

B-D. A representative plot of worm speed over time under conditions where satiety quiescence is impaired with **B)** wild-type worms nonfasted on high quality food, **C)** wild-type worms fasted and refed on poor quality food, **D)** worms with *egl-4* loss-of-function mutation fasted and refed on high quality food.

E. A 20 minute timecourse of worm speed after fasting and refeeding on high quality food shows that worms seem to alternate between states of activity (black bar) and inactivity (gray bar). For this simple determination of active and inactive, states were determined subjectively.

F. The mean speed of the worm in each experiment was calculated and the average taken to give the mean speed of worms for each of the four conditions listed above (1A-D).

Following Kruskal-Wallis ANOVA ($p < .001$ for both), $**p < .01$, $***p < .001$ by Mann-Whitney *U*-test.

quality food and small bacteria are high quality food. To modulate food quality, we treat the bacteria with aztreonam to inhibit cell wall separation which results in long strands of connected bacteria (Figure 2A, B). This has previously been done to distinguish odor from nutritional signaling effects and has been shown to affect worm behavioral state (39,90). To prepare the bacteria as poor quality food, we use a shorter incubation time than these previous studies. I verified that worms are still able to ingest bacteria treated this way by using HB101 that expresses mCherry and viewing fluorescence through the gut.

Previous studies (38,39) quantified two characteristics of the worm's motion: speed and change of direction (referred to as "curvature" by Ben Arous et al. (39) and "turning" by Fujiwara et al.(38)). Change of direction cannot be measured accurately when the worm is moving slowly. To solve this problem, we measured speed, change of speed (tangential acceleration), reversal, and turning (radial acceleration) from each set of three successive points (see Motion characteristics in Methods). To illustrate motion characteristics of roaming, dwelling and quiescence, we show three short movie segments that illustrate typical roaming, dwelling, and quiescence behavior (Figure 3; see Statistically typical tracks in Methods). We found two differences between roaming and dwelling. First, consistent with Fujiwara et al. (38), reversals were much more frequent in dwelling. Second, during dwelling acceleration was correlated with speed. During roaming, in contrast, there was no obvious correlation of speed with acceleration.

Our results showed mostly low radial acceleration during dwelling, which appeared to contradict its previous description as the state with frequent changes in direction. However, after calculating speed and absolute angular change in direction across all our

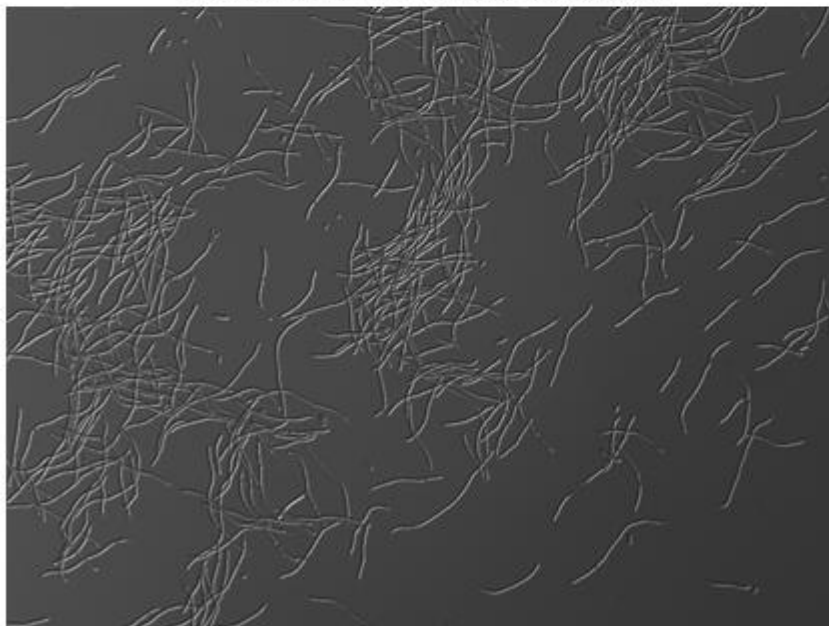
Figure 2**A**HB101 *E. coli***B**HB101 *E. coli* treated with aztreonam

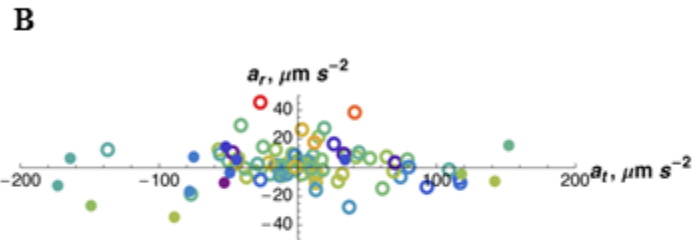
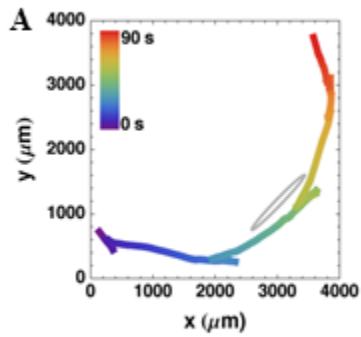
Figure 2. Treating bacteria with aztreonam increases bacterium size.

A. Nontreated *E. coli* strain HB101.

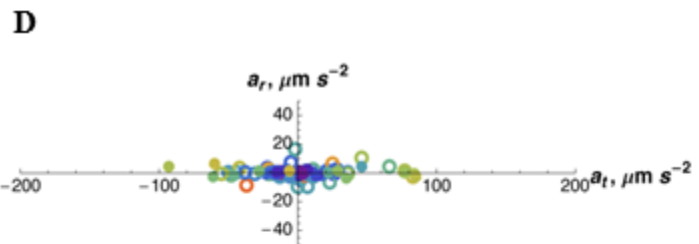
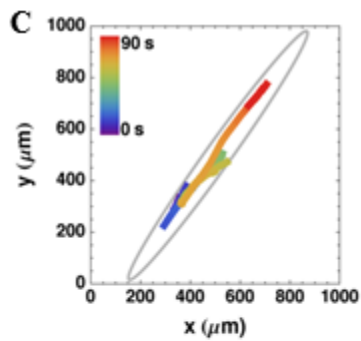
B. *E. coli* strain HB101 treated with aztreonam form long strands, increasing its size.

Figure 3

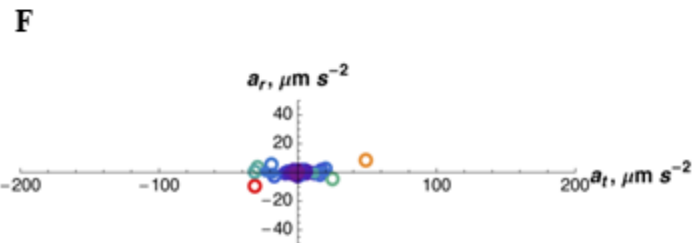
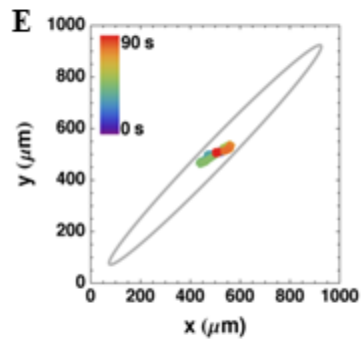
Roaming



Dwelling



Quiescence



0 s_{max} ● Reversal ○ Nonreversal

Figure 3. Motion characteristics of roaming, dwelling, and quiescence.

A-F. Short movie segments illustrating statistically typical roaming (**A, B**), dwelling (**C, D**), or quiescence (**E, F**) (chosen as described under Statistically typical tracks in Methods) were analyzed to determine speed, acceleration, and reversal at each time. The tracks are shown in **A, C, and E**. Time is indicated by color. Note the difference in scale between **A** and the other two. The grey ellipses are 1.2 mm long \times 0.1 mm wide, about the size of the worm.

B, D, F: Tangential and radial acceleration are plotted on the x and y axes. Speed is indicated by color, with the lowest and highest speeds indicated by purple and red. (Color is normalized within each track, so that, for instance, red points within the dwelling plot represent a lower speed than red points in the roaming track.) Reversal is indicated by filled circles, and nonreversal by empty circles.

tracks, we found that change in direction is almost entirely reversal. “Change in direction” conflates two distinct behaviors, reversal and turning. The large average angles reported previously for dwelling and roaming (39) are because a majority of nonreversals—angles near 0° —are averaged with a substantial minority of reversals—angles near 180° (Figure 4).

To capture the information available in the time course of behavior, we used a Hidden Markov Model (HMM). Behavioral state cannot be reliably determined by looking at a single point in time. For instance, although a dwelling worm moves most of the time, there are time points at which no detectable movement occurs. By themselves, these cannot be distinguished from quiescence. However, this ambiguity can be resolved by looking at the time course of behavior. A dwelling worm is still only at isolated points in time, while a quiescent worm remains so almost continuously. In HMM analysis the state inferred at one time depends, not just on behavior at that time, but also on states immediately before and after (Figure 5A, B).

We deduced the characteristic behavior of roaming, dwelling, and quiescent worms from records acquired under conditions in which worms have been reported to spend most of their time in just one of these states (see Standard state fits in Methods). Figure 5C shows the result of such a fit to a recording of a well-fed wild-type worm on good food. Although there were brief periods during which behavior was ambiguous (e.g., just before 1000 s, when there is a ~75% probability of dwelling and ~25% of quiescence), at most times one state was identified with close to 100% confidence.

Figure 4

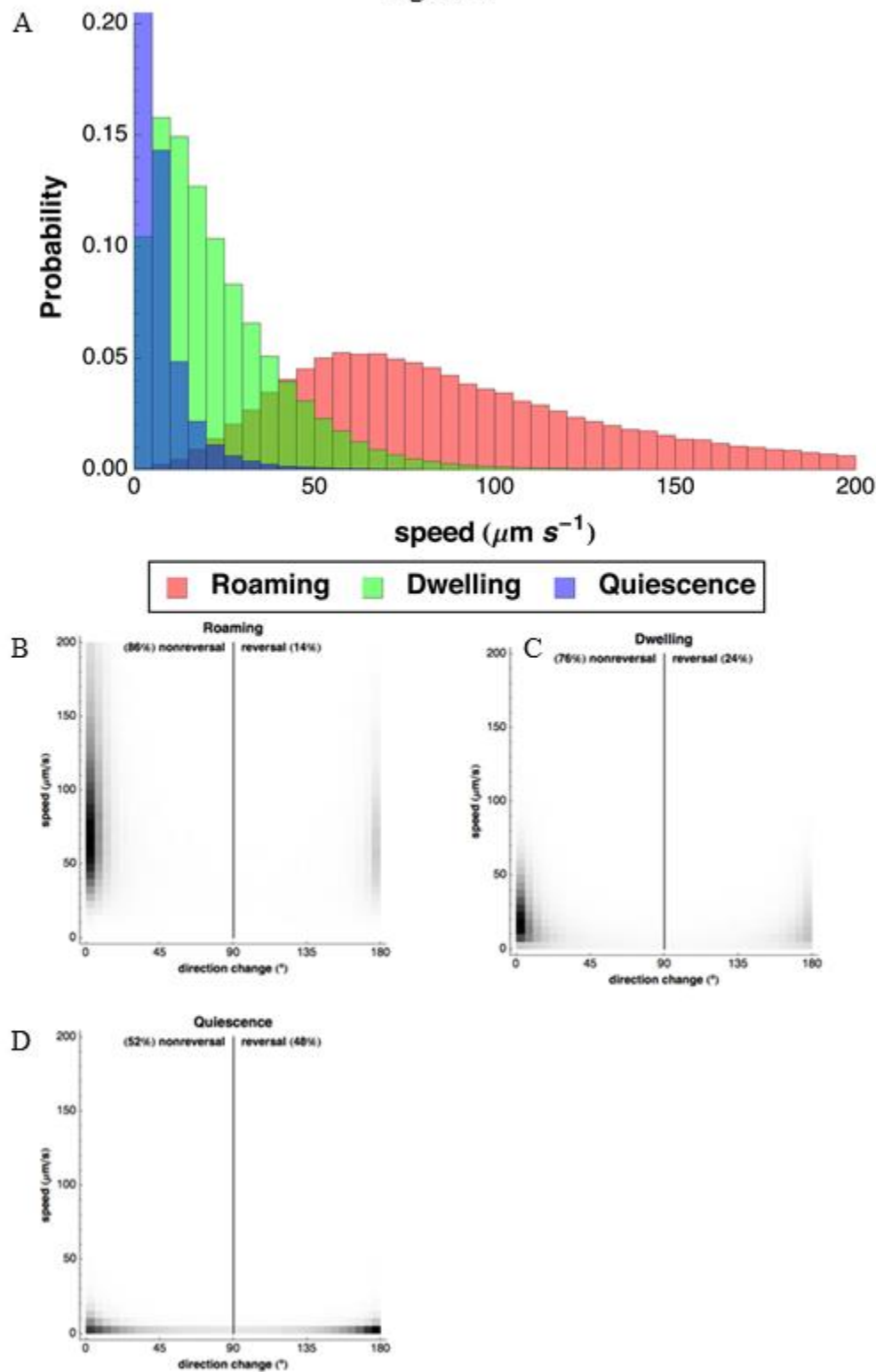


Figure 4. Speed histograms, speed, and direction change for roaming, dwelling, and quiescent worms.

A. 363 tracks were analyzed by open-loop fits to the standard roaming, dwelling, and quiescent state descriptions defined by standard state analysis, then the time points were selected at which one state was assigned with at least 99% probability. At each such point we determined center of mass speed and change in direction. Blue is quiescence, green dwelling, and red roaming. To allow all three distributions to be clearly seen, the plot was cut off at 0.2. The probability of $s < 5 \mu\text{m s}^{-1}$ for quiescence is 0.76.

B-D. For each point classified as described in the legend to **A**, we determined speed and absolute change in direction of the center of mass. In all states the direction change is concentrated near 0° and near 180° , with a wider spread at low speeds as expected from the difficulty of accurately measuring directions when movements are small. Our motion analysis classifies as reversals those points with a direction change greater than 90° .

Figure 5

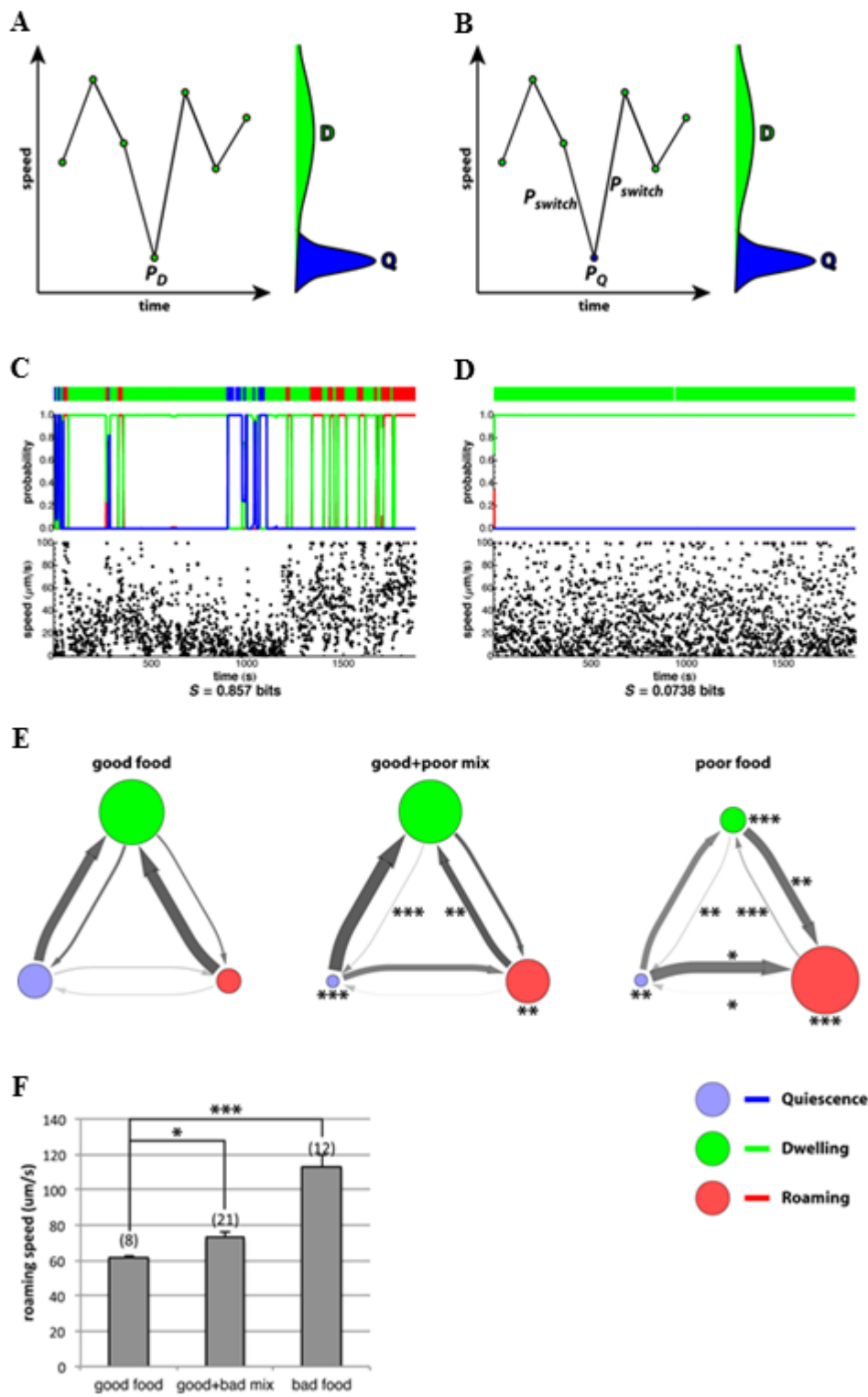


Figure 5. Hidden Markov Model analysis, standard state fits.

A, B. A simplified explanation of how HMM analysis uses both time and behavior to determine state. The plots show a hypothetical record of speed vs time. The bell-shaped green and blue curves at the right of each plot show the probability for a dwelling or a quiescent worm to move at a given speed. The distributions overlap, because while dwelling worms usually move faster than quiescent worms, at some time points they move as little as a quiescent worm. (Although a quiescent worm doesn't move at all, its measured speed will usually be positive because of small errors in the measurement of its position.) The problem is to determine what state the worm was in at the central time point, where it did not move. Looking at this point alone, one would conclude that the worm was probably quiescent, because the probability for a quiescent worm to move so slowly (P_Q ; panel B) is much higher than the probability that a dwelling worm will do so (P_D ; panel A). However, the behavior of the worm immediately before and immediately after is inconsistent with quiescence. Therefore, if the worm is quiescent at the central time point, it must have switched from dwelling to quiescence immediately before and must switch back immediately after. The probability that the worm is quiescent is therefore $P_{switch}^2 P_Q$. If the time between points is small, the probability of a switch, P_{switch} , is a small number, and $P_{switch}^2 P_Q \ll P_D$. The worm is thus correctly inferred to be dwelling. The actual analysis is more complicated, since other motion characteristics than speed are used, and a probability is assigned to each state at each time point.

C. The results of standard state fit to a wild-type track. The lower plot shows speed; red,

Figure 5 continued.

green, and blue lines in the upper plot show probability of the roaming, dwelling, and quiescence state at each point in time.

The color bar at the top summarizes the probabilities. (The small gap is a brief period of missing data.) The change in behavior with time is most easily seen by looking at the frequency of very low speed ($<20 \mu\text{m/s}$). Such time points are a majority in quiescence, a substantial minority in dwelling, and almost absent in roaming. Most time points are assigned to a single state with near 100% probability, and the worm spent a substantial amount of time in each of the three. This is reflected in the high excess entropy, 0.857 bits.

D. The results of a similar fit to the same data as in **C**, but scrambled into random order.

The three-state fit did not have substantially more information than a single behavioral state, as shown by the very low entropy (S).

E. Rate graphs summarizing state probabilities and transition rates between states based on analysis of well-fed wild-type worms on either good food (*E. coli* HB101), poor food (HB101 treated with aztreonam) or a mixture of good and bad. The area of each circle is proportional to the amount of time worms spend in that state (red = roaming, green = dwelling, blue = quiescence). Thicker arrows represent faster switching from one state to another. Darker arrows are more accurately measured, lighter grays represent less accurate measurements, based on variability from one worm to another. $*p < 0.05$, $**p < 0.01$, $***p < 0.001$, different from good food, Mann-Whitney U -test. Thus, for instance, worms switch from dwelling to roaming more rapidly ($p < 0.01$) on poor food than on good and spend more time roaming ($p < 0.001$). Number of worms for each graph as in **F**.

Figure 5 continued.

F. Mean speed of roaming worms. These data are based on the same tracks as **E.** Number of worms in each experiment is shown above the bar. * $p < 0.05$, *** $p < 0.001$, Mann-Whitney U -test.

We developed a statistic, excess entropy, to quantify the extent to which the analysis helped to explain behavior. The fit in Figure 5C had an entropy of 0.86 bits. (The maximum possible is $\log_2 3 \approx 1.58$.) To test if the fit truly detected coherent time-dependent changes in behavior, we scrambled the data and repeated the fit. Figure 5D shows an example of one such fit to scrambled data. No state changes are detected, and the entropy is only 0.074 bits.

Using this analysis, we confirmed and extended earlier results. For instance, low-quality food suppresses quiescence (20) and promotes roaming (20,29). We confirmed these results (Figure 5E). Further, our analysis allowed us to estimate the rate at which worms switch from one state to another. The suppression of quiescence was explained mainly by a decrease in the rate at which worms switch from dwelling to quiescence (Figure 5E).

A simple hypothesis for the control of locomotory behavior is that food quality and other conditions affect only the rates at which worms switch between states. Under this hypothesis worms on poor food would spend more time roaming, but during the time they spend roaming, worms would behave the same on good food and on poor food. The alternative is that the behavior of a worm depends not only on the state it is in, but also on conditions. Under this hypothesis roaming worms might behave differently on good food and on poor food.

To test these hypotheses, we compared the motions of worms in the same state under different conditions. Figure 5F shows an example: the speed of worms on good food, poor food, or a mixture, measured only during the time they spent roaming. The simple

hypothesis was decisively rejected. Roaming worms on poor food moved faster than roaming worms on good food and roaming worms on mixed food, which was also observed by Ben Arous et al. (39), who reported that roaming worms move faster on poor food.

2.2 Unbiased state discovery

The observation that the behavior of a roaming worm depends on conditions such as food quality raised a difficult question: how are roaming, dwelling, and quiescence defined? Above we claimed that roaming worms moved faster on poor food. This claim is correct, if roaming is defined by the motions of worms under conditions that have been reported to promote roaming. However, speed is one of the characteristics that distinguishes dwelling and roaming. If poor food caused dwelling worms to move faster, they might be classified as roaming. If poor food in addition caused dwelling worms to reverse less and to accelerate less, any method that deduces behavioral state from these characteristic motions would classify the behavior as roaming.

To address this problem, we developed an unbiased analysis in which state characteristics are derived directly from the behavior of a single worm (see Unbiased closed-loop fits in Materials and methods). Our fits of 363 recordings yielded a total of 1083 state descriptions from 357 three-state and 6 two-state fits. A state description is the list of seven parameters that specify such behavioral characteristics as the probability of reversal, the mean speed, and the correlation between speed and acceleration. Each state is

thus a point in a seven-dimensional space. Interestingly, however, most of the points lay close to a plane—93% of the variance is captured in two dimensions. It was thus possible to plot them in two dimensions while preserving most of their geometric relationships.

Figure 6 shows such plots.

We were able to identify regions of the plot that correspond to roaming, dwelling, and quiescence by considering their motion characteristics and by comparing our results with published results. The arrangement of states is roughly triangular (Figure 6G). The location corresponding to immobility is near the lower left, so this is the direction of quiescence. Speed increases towards the upper right of the plot, while reversal increases towards the lower left. Thus, upper right is the direction of roaming, which is characterized by high speed with few reversals. Covariance of acceleration and speed increases towards the upper left, which is thus the direction of dwelling.

To more precisely identify regions with states, we looked at the results of specific experiments. Wild-type worms fasted for twelve hours then refed with good food for three hours alternate between quiescence and dwelling (20). (When not observed, worms so prepared spend most of their time quiescent, but watching them disturbs them in some unknown way, causing them to wake and dwell (20). Our recording conditions allowed some quiescence, but were disturbing enough that the worms also dwelled.) Each such worm had two high-probability states, one in a region close to the lower half of the left side of the triangle, and another near the center (Figure 6A), which we thus identified as quiescence and dwelling, respectively. On poor food wild-type worms roam. They spent most of their time in states near the right vertex (Figure 6B). The states of *egl-4(lf)* mutant

Figure 6

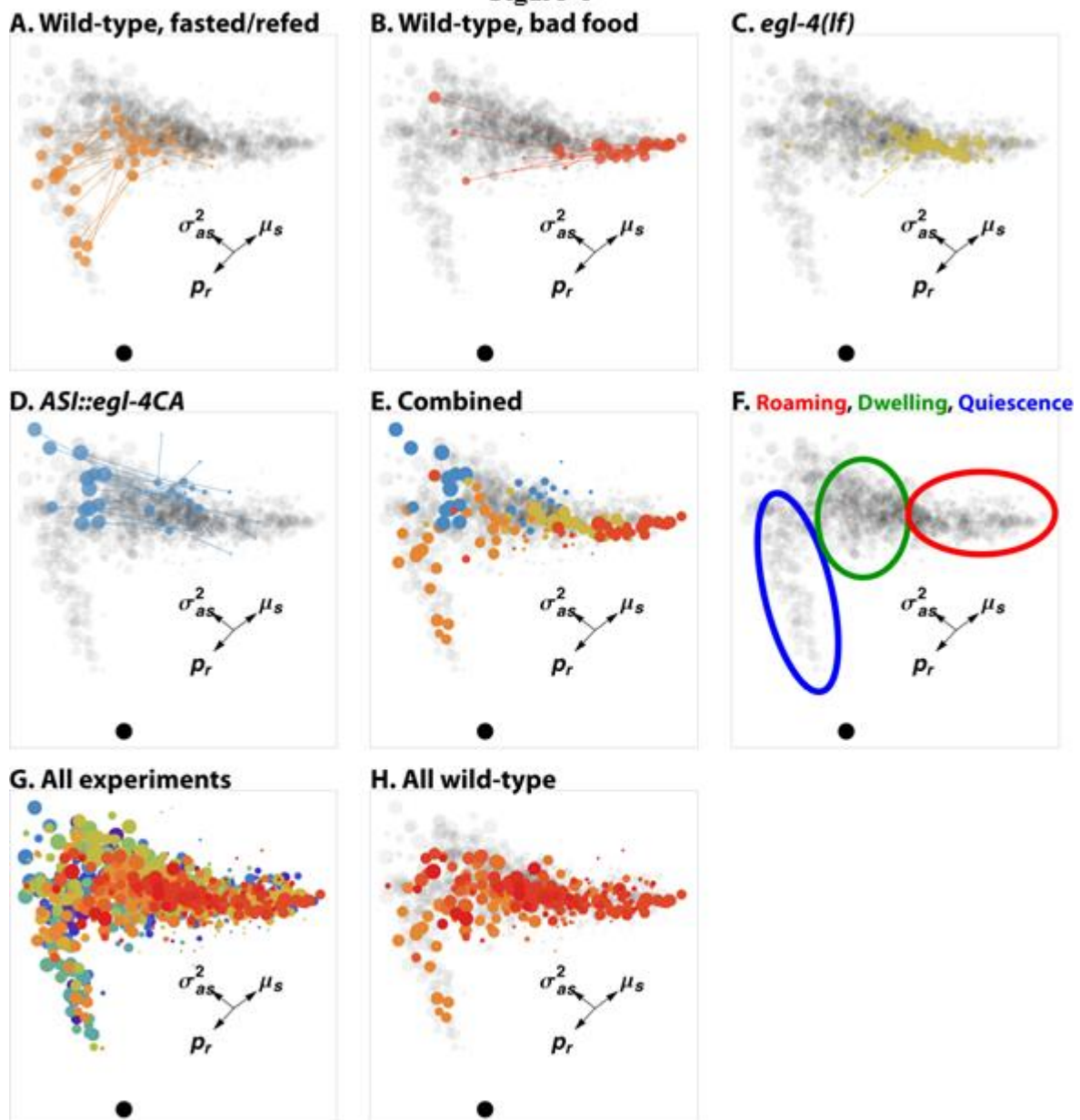


Figure 6. Geometry of behavioral states.

This figure shows the two-dimensional arrangement of behavioral states discovered by unbiased open-loop fits. Each circle (except the black one near the bottom of each panel, which represents complete immobility) represents a single state from a single worm. The area of the circle is proportional to the amount of time the worm spent in that state. The gray background in **A–F** and **H**, representing all states discovered in all experiments, is shown for context. States are colored by experiment; the same colors are used in panels **A–E** and **G–H**. Arrows show the directions in which three of the seven state parameters increase. P_r is the probability of reversal, μ_s is mean deskewed speed, and σ_{as} is the covariance of deskewed speed and acceleration.

A–D. States discovered in four experiments. Lines join states discovered in the same worm.

A. 14 wild-type worms, fasted for 12 hours, refed on good food (*E. coli* HB101) for 3 hours, then recorded on good food.

B. 12 wild-type worms, grown on good food and recorded on poor food. (Poor food is HB101 treated with aztreonam, which prevents cell division (39).)

C. 12 mutant worms lacking cGMP-dependent protein kinase (PKG, encoded in *C. elegans* by *egl-4* (38)), grown and recorded on good food.

D. 12 transgenic worms that express constitutively active PKG in ASI neurons, grown and recorded on good food.

E. States from the four previous experiments plotted together.

Figure 6 continued.

F. Regions of the triangle can be identified as roughly corresponding to roaming, dwelling, and quiescence, as described in the text.

G. All behavioral states discovered in 49 experiments on 363 worms.

H. States from all experiments on wild-type worms (80 worms total). These experiments differ only in whether the worms were well-fed or starved and refed, and in the quality of food on which they were recorded.

worms, which spend most of their time roaming even on good food (29), were in the same general region (Figure 6C). Worms engineered to express constitutively active cGMP-dependent protein kinase in ASI neurons showed an unusual pattern that was never seen in wild-type worms. They alternated between two states, a less probable one near the boundary between dwelling and roaming, and a more probable one near the upper left corner of the triangle. We call the latter state hyperdwelling, since it exhibits the characteristics of dwelling even more strongly than a dwelling wild-type worm. Figure 6F summarizes the regions corresponding to roaming, dwelling, and quiescence.

2.3 Are there discrete locomotive behavioral states?

We were surprised that we did not find discrete, well-separated clusters corresponding to roaming, dwelling, and quiescence. Rather, as shown in Figure 6G, the observed states filled most of the triangle, sparing only the region between quiescence and roaming. This suggests that our previous view, that the worm has available to it three distinct patterns of locomotive behavior, might be too simple. Instead the worm may be able to continuously tune its behavior between these three patterns.

We considered three alternative explanations for the failure to observe discrete clusters of states. First, the clusters might exist but be blurred by noise. There is error in every measurement. Perhaps the errors were so great as to spread the clusters until they merged with each other, giving a false appearance of continuity. This explanation was refuted by looking at single experiments. Figure 6A-D clearly show well-defined clusters

of states. Each of A and D, in fact, shows two well-separated clusters, and each worm in those experiments alternated between a state in one cluster and a state in the other. We clearly had the ability to resolve distinct patterns of behavior. Figure 6E emphasizes this by showing that the states discovered in the experiments of A-D occupy six distinct, well-defined positions.

Figure 6E suggests a second possible explanation for the lack of clusters. Although 9 of our 49 experiments were done on wild-type worms, the rest were done on various mutant genotypes. Perhaps normal worms do have discrete roaming, dwelling, and quiescence states, but the unnatural behavioral patterns of mutants fill up the blank regions between the wild-type states. In fact, it was obvious that without the ASI::*egl-4CA* and *egl-4(lf)* experiments, the wild-type states of Figure 6A, B would form three discrete clusters (red and orange states in Figure 6E). To test this, we plotted all the states discovered in experiments on wild-type worms (Figure 6H). Even when we looked only at wild-type, discrete clusters were not evident.

A third possible explanation for our failure to identify clusters is more complicated. The plots in Figure 6 show the disposition of states in two dimensions, but the actual state space is seven-dimensional. Perhaps roaming, dwelling, and quiescence are separated from each other in the full seven-dimensional space, but this separation is lost when they are projected onto a plane. While we cannot entirely exclude this possibility, we found no evidence for it. It is somewhat implausible on its face, since the two dimensions plotted capture 93% of the variance—any additional separation could occur only in the remaining 7%. We examined state plots in 3 dimensions and looked at projections onto planes

containing each of the seven dimensions and found no evidence of discrete clusters. In addition, we attempted to automate the search for clusters using hierarchical cluster analysis based on all seven state characteristics (Figure 7). The results were disappointing. While by design cluster analysis always finds clusters, the state clusters were excessively sensitive to the details of the algorithm (different distance measures and linkage methods often produced widely different clusters) and to the data included (during the course of this work clusters often changed radically with the addition of a few new recordings). Furthermore, the clusters failed basic experimental consistency criteria. For instance, if the red, green, and blue clusters in Figure 7 corresponded to roaming, dwelling, and quiescence, we would expect that fasted and refed wild-type worms would alternate between a blue state and a green state. Some of them did, but in others the two main states were both green. We do not believe that the clusters identified by cluster analysis have any biological reality.

2.4 Behavioral states are arranged in a triangle

Looking at the arrangement of all states (Figure 6), we were struck by the impression that they fill out most of a triangle. To test this impression, we used a test recently described by Shoval et al. (91). We compared the area of the smallest polygon that contains the states to that of the smallest triangle that contains them (Figure 8A). If they were really arranged in a triangle, the smallest polygon that contains them would be a

Figure 7

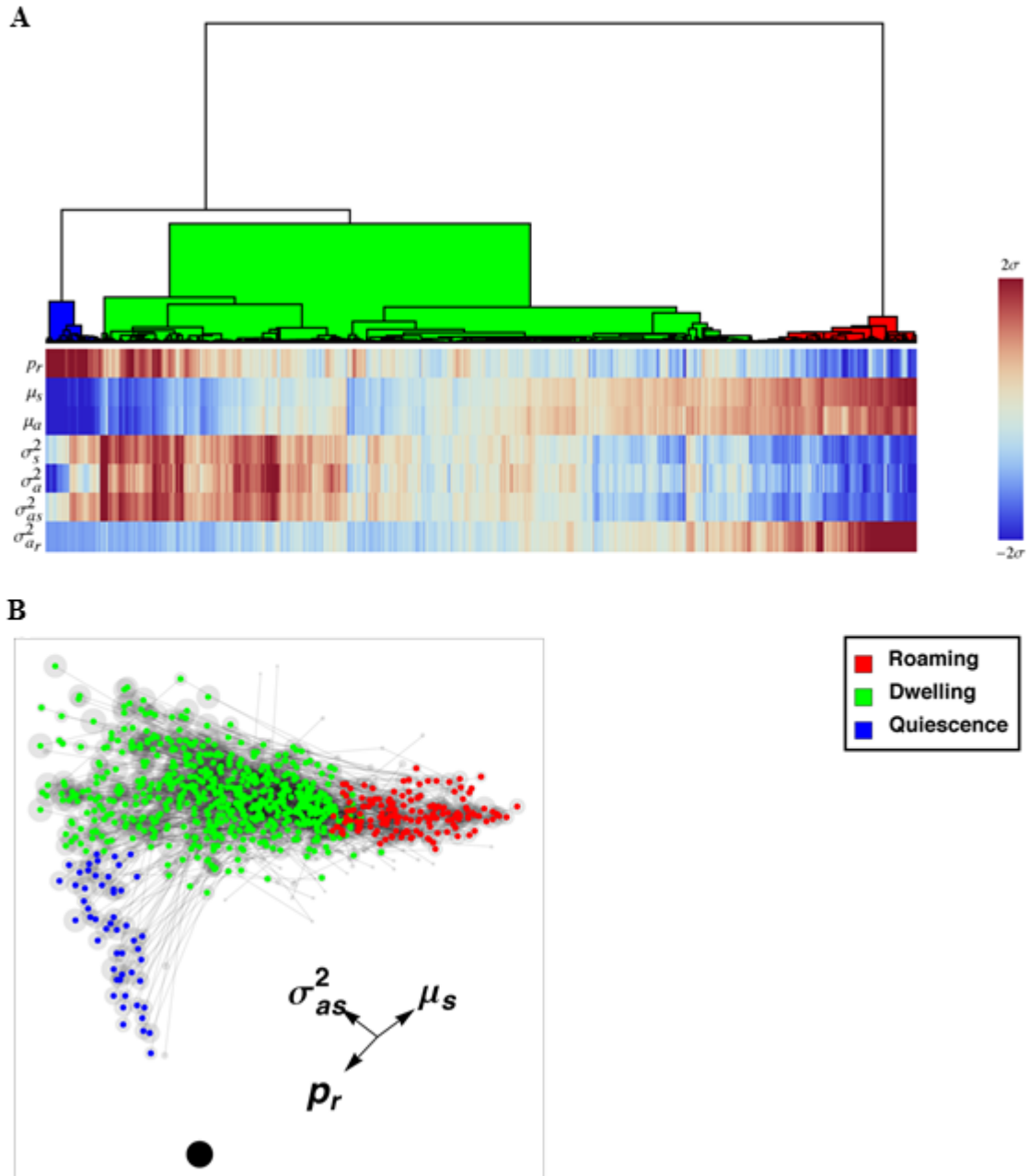


Figure 7. Hierarchical cluster analysis of states.

A. Hierarchical clustering of state descriptions resulting from unbiased closed-loop fits.

832 of the 1083 states plotted in Figure 6G, those with probability $\geq 10\%$, were clustered.

The seven values constituting each description are plotted in the heat map below the dendrogram, and the top three clusters are highlighted in blue, green, and red.

B. Identification of clustered states. States, plotted as in Figure 6, are identified by red, green, and blue dots according to which cluster they belong to.

Figure 8

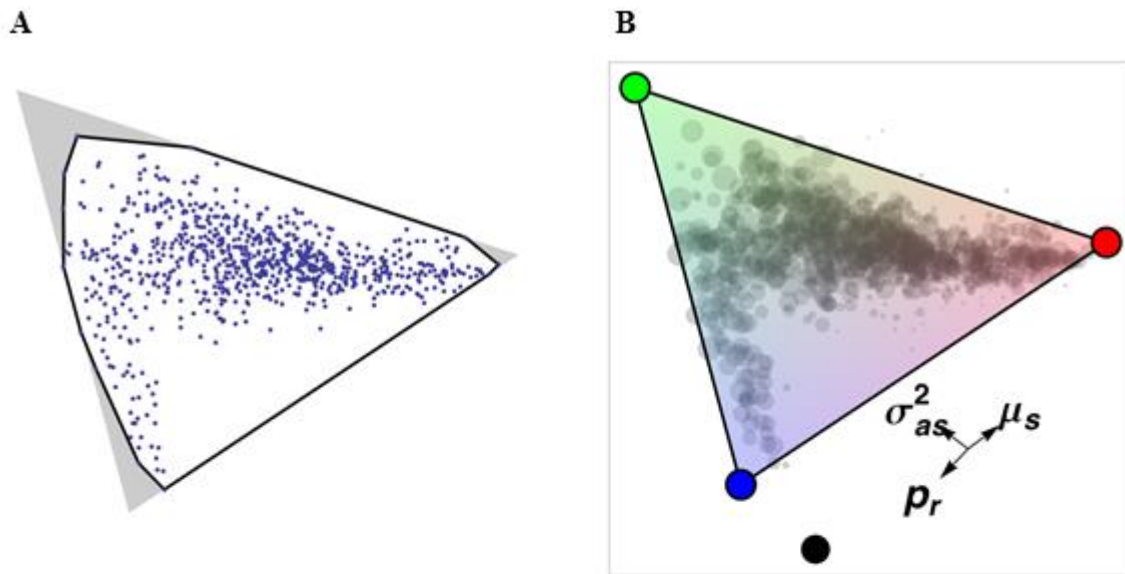


Figure 8. Behavioral states are arranged in a triangle.

A. Each of the 832 states with probability greater than 10% is plotted in two dimensions as in Figure 6. The black line is the smallest polygon that contains all of them (the convex hull). The area of this polygon is 90.5% that of the smallest triangle containing them, significantly greater than that expected if they are not constrained to a triangle ($p < 10^{-5}$). The corresponding figure for a test using all the states, not just those with probability greater than 10%, is 90.8% ($p < 10^{-5}$).

B. An interpretation of the triangular state space. We suggest that the locomotive behavioral patterns available to a worm can be any mixture of three archetypal patterns, represented as red, green, and blue circles. Like primary colors, these mix to form a triangle of possibilities.

significantly greater than that expected for a random arrangement of points at $p < 10^{-5}$.

2.5 Verifying previous results with TOBO

To better compare different strains and conditions of worms using Hidden Markov Model analysis we calculated the percent time that worms spent in each behavioral state based on the most likely behavioral state that the worm is in over time (closed-loop fits, pure play analysis). Repeating what we had initially seen by looking at speed over time, average speed, and time at low speed, worms fasted and refed on high quality food show enhanced quiescence compared to worms that are not fasted, fasted and refed on poor quality food, and *egl-4(lf)* worms that are fasted and refed (Figure 10). In addition, this analysis finds that *egl-4(gf)* worms show enhanced quiescence under conditions where quiescence is not normally enhanced (nonfasted, which we had previously reported (20)) and was further enhanced when worms are fasted and refed (Figure 9).

At this point, we have established this analysis and behavior as a highly quantitative method of determining worm behavioral state over time. The limitation was that we could only record one worm at a time. This limited the experimental throughput that we were capable of and precluded concurrent controls. Fortunately, we were in possession of a worm surveillance platform custom built by a former member of the Avery lab, Dr. Boris Shtonda, which holds nine cameras. We replaced the cameras (off the shelf security cameras) with high resolution cameras fitted with macro lenses, changed condensers for diffusers, and incandescent lights for LED light strips (Figure 10). We

Figure 9

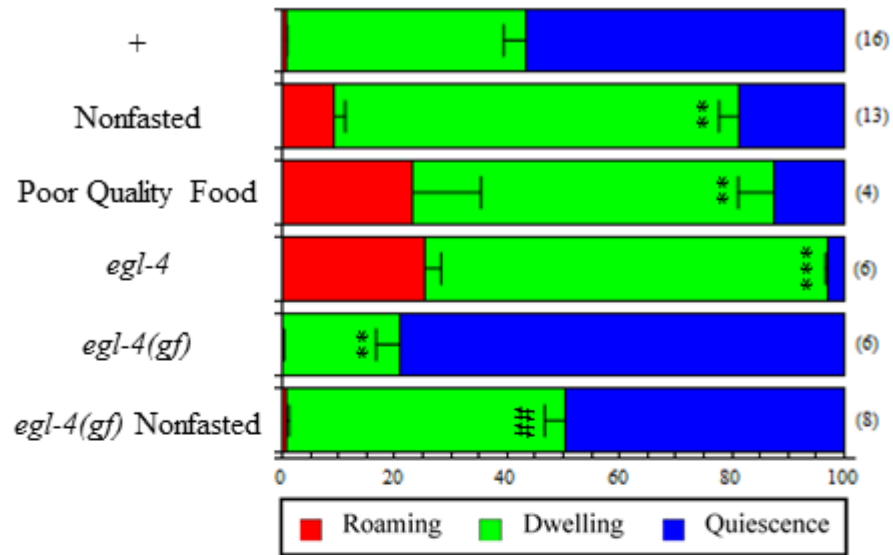


Figure 9. Locomotion tracking and HMM analysis repeats previous findings in satiety quiescence behavior.

Wild-type worms fasted and refed on high quality food spend about 60% of their time in the quiescent behavioral state. This is reduced in wild-type worms nonfasted or fasted and refed on poor quality food. Worms with *egl-4* loss-of-function mutation show less time in the quiescent behavioral state after fasting and refeeding on high quality food. Worms with *egl-4* gain-of-function mutation show enhanced satiety quiescence either fasted and refed or nonfasted. Number of tracks analyzed for each condition shown to the right of the data. Percent time in each behavioral state was determined by Pure Play Analysis. $**p < 0.01$, $***p < 0.001$ compared to wild-type fasted-refed, $##p < .01$ compared to wild-type nonfasted Mann-Whitney *U*-test following Kruskal-Wallis ANOVA ($p < .001$).

Figure 10

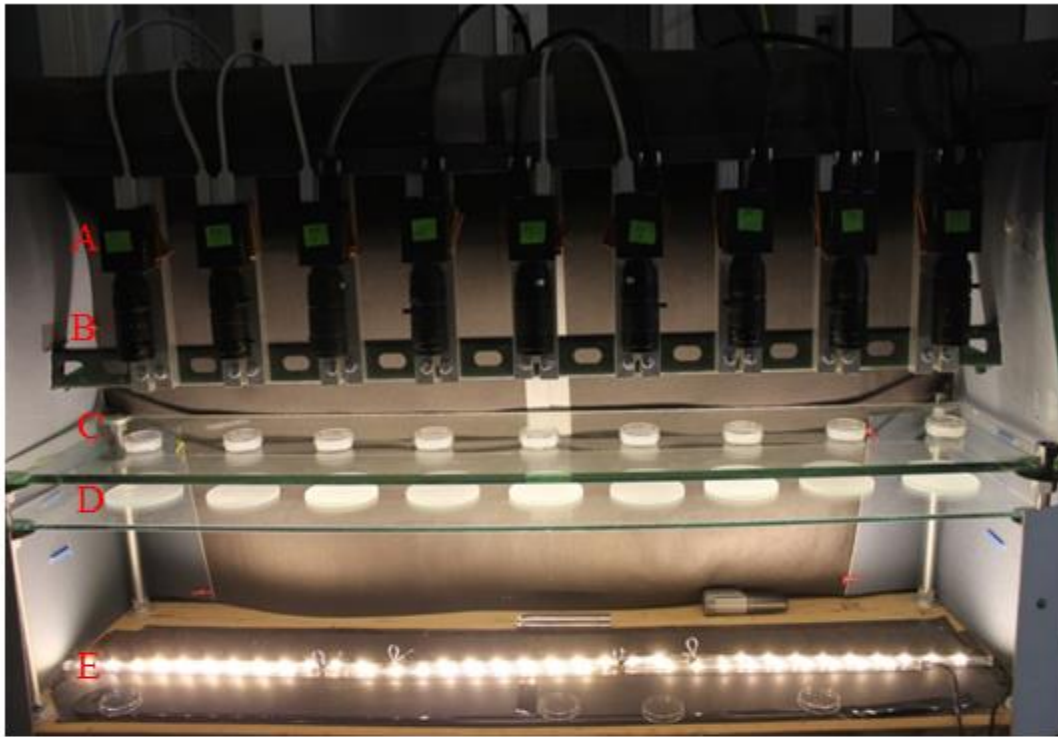


Figure 10. TOBO.

Custom built locomotion tracking platform with nine cameras.

A. Point Grey Grasshopper cameras.

B. Macro lenses.

C. A single worm was placed on a plate for each recording.

D. Semi-translucent diffusers.

E. LED light strips were used for illumination.

have named this system TOBO (TOM and BORIS).

One concern of using aztreonam to modulate food quality is whether the change in worm behavior is due to the change in food quality or because the worms are sensitive to the drug. To test this, we assayed worms on nontreated bacteria, bacteria incubated with aztreonam, and bacteria with aztreonam added after incubation. Both nonfasted and fasted-refed worms show decreased quiescence and increased roaming when fed on aztreonam treated bacteria (this is the same condition referred to as ‘Poor quality food’ above). However, worms fed on bacteria with aztreonam added after the incubation period showed no difference in behavioral state from worms on nontreated bacteria both in fasted-refed and nonfasted conditions, showing that the effect on behavior is due to the worms responding to the bacteria and not aztreonam itself (Figure 11A).

We additionally tested whether we could create an intermediate quality food by mixing high quality and poor quality food. Mixing 9:1 poor quality to high quality (v/v after the bacteria was centrifuged and diluted), showed this intermediate effect. In both conditions this suppressed roaming compared to worms on aztreonam treated bacteria and suppressed quiescence compared to worms on non-treated bacteria (Figure 11B).

2.6 TGF β regulation of satiety quiescence

Having developed a method to identify satiety quiescence over time, we then were able to ask questions about what regulates this behavioral state. Mutations in the worm TGF β signaling pathway impair satiety quiescence (20). Our locomotion tracking and HMM

Figure 11

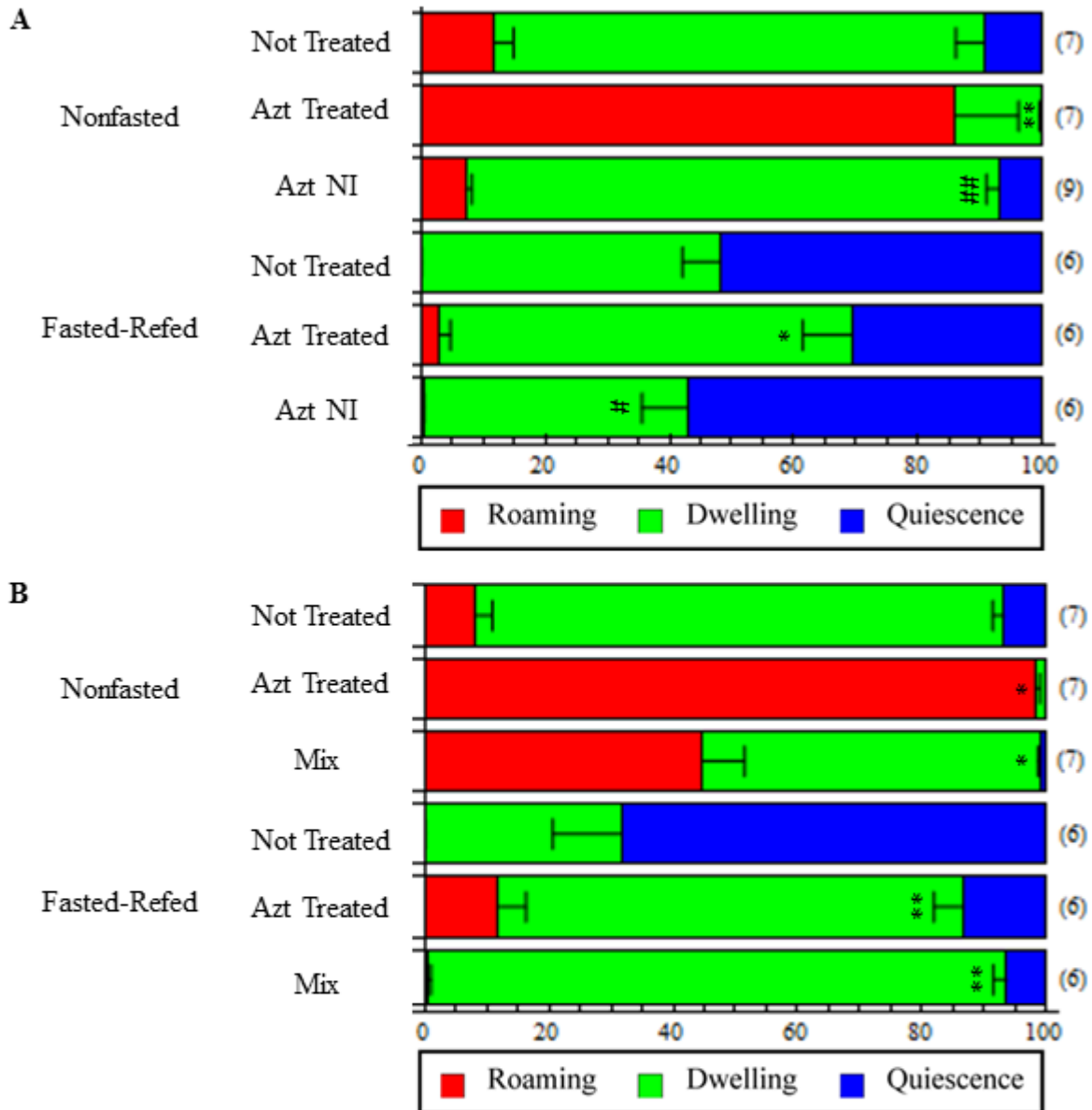


Figure 11. Aztreonam treated bacteria acts as poor quality food.

Standard state probabilities of worms which were concurrently assayed with wild-type worms using TOBO.

A. Aztreonam was either not added to bacteria (Not Treated), incubated with the bacteria (Azt Treated), or added after the incubation (NI, Not Incubated). Both nonfasted worms as well as worms fasted and allowed to fully refeed on the indicated food source show decreased quiescence and increased roaming only with bacteria incubated with aztreonam. Adding aztreonam after incubating the bacteria has no effect, indicating that worms are responding to the effect aztreonam has on the bacteria and not the drug itself.

B. Mixing not treated bacteria with aztreonam treated bacteria gives an intermediate food quality. After being centrifuged and diluted, aztreonam treated bacteria was mixed with nontreated bacteria (9:1 treated:nontreated, v/v) to create a mixed food. This food condition suppresses roaming in both nonfasted and fasted-refed worms compared to worms on aztreonam treated bacteria. Worms on mixed food show also show less quiescence than worms on nontreated bacteria.

Number of tracks analyzed for each condition shown to the right of the data. Percent time in each behavioral state was determined by Pure Play Analysis. Experiments were done concurrently using TOBO. * $p < 0.05$, ** $p < 0.01$ compared to wild-type not treated, ### $p < .01$ compared to wild-type aztreonam treated Mann-Whitney U -test following Kruskal-Wallis ANOVA ($p < .001$).

analysis repeated this finding, as *daf-7* worms show decreased time in quiescence after both fasting and refeeding and nonfasted (Figure 12A). Since *daf-7* is expressed in ASI, we also tested ASI ablated worms, generated by expression of recombinant caspase (92,93) and found that these worms show a similar decrease in quiescence both nonfasted and fasted-refed (Figure 12A). While ASI ablation has been reported to cause constitutive dauer entry (83,84), we do find a small percent of escapers that undergo the normal reproductive life cycle allowing us to maintain a population and test them in our assay. In both *daf-7* and ASI ablated worms, quiescence is decreased and dwelling is increased. Our HMM analysis has shown that this is due to *daf-7* and ASI- worms switching from quiescence to dwelling more rapidly than wild-type worms (Figure 12B).

Because the HMM analysis is locomotion based but satiety quiescence is the cessation of both movement and feeding, we also quantified food intake. We accomplished this by fasting worms, refeeding them on mCherry expressing HB101, and quantifying fluorescence through the gut. Corresponding to the locomotion data showing decreased quiescence, *daf-7* and ASI- worms both have increased food intake (Figure 12C). Since mutations anywhere in the TGF β signaling pathway should impair quiescence, we also tested food intake of worms with a mutation in *daf-1*, *daf-8*, or *daf-14* and found that they have a similar increase in food intake as *daf-7* worms (Figure 12C). Since *daf-7* expression is dependent upon the guanylyl cyclase *daf-11* (89), we additionally tested *daf-7* regulation by cGMP. We accomplished this by using a transgenic strain expressing *daf-7* fused to mCherry under the *daf-7* promoter and quantifying the levels by measuring fluorescence. Fasting worms for 12 hours and refeeding for 3 hours on

Figure 12

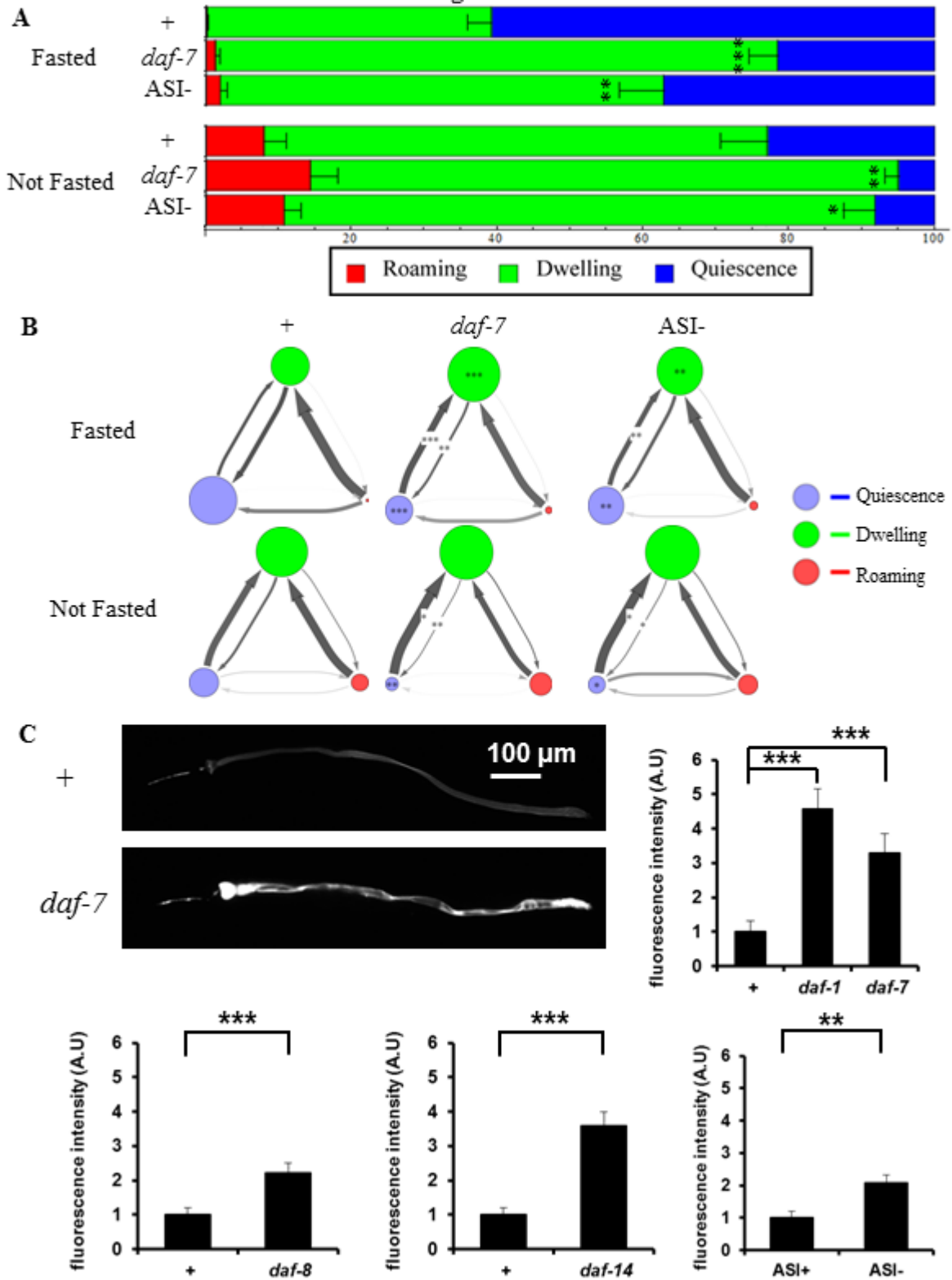


Figure 12. TGF β in ASI neurons promote the switch from dwelling to quiescence.

A. Standard state probabilities of wild type, ASI ablated worms and *daf-7* mutants show inhibition of satiety quiescence both fasted and fully refed as well as nonfasted. Data was collected before implementing TOBO and so was not done concurrently. Wild-type fasted-refed and nonfasted data is repeated from Figure 9. $*p < .05$, $**p < .01$, $***p < .001$ compared to wild-type by Mann-Whitney *U*-test.

B. DAF-7 from ASI regulates transition rates from dwelling to quiescence. Transition rates among states of wild type, ASI ablated worms and *daf-7* mutants. Each diagram shows state probabilities and transition rates from one experiment after standard state fits. Each circle represents a state: light gray for quiescence, medium gray for dwelling, and black for roaming. The area of the circle is proportional to the probability of the state under those conditions. Each arrow represents a transition from one state to another. Thicker arrows represent higher transition rates. Darker arrows represent rates measured with high accuracy, paler arrows rates measured with poor accuracy. $**p < .01$, $***p < .001$, by Mann-Whitney *U*-test.

C. Representative pictures of wild-type and *daf-7* worms after 12 hours fasting and 3 hours refeeding on mCherry expressing HB101. *daf-7* show higher fluorescence reflecting more food intake. Quantification of fluorescence of canonical TGF β signaling pathway mutants and ASI ablated worms eat more than wild-type worms after fasting and refeeding as all show higher fluorescence.

HB101 strain of *E. coli* (the same experimental design under which we find enhanced satiety quiescence increases DAF-7 levels (Figure 13). Fasting worms for 12 hours and placing them on 8-Br-cGMP treated plates (1 mM) in the absence of food caused a similar increase (Figure 13). However, nonfasted worms did not show a change in DAF-7 levels after treatment with 8-Br-cGMP for 3 hours (Figure 13). Additionally, we did not see a decrease in *daf-7::mCherry* fluorescence in starved worms compared to well-fed worms as had been previously reported (50). This could be due to mCherry being a very stable protein and so not being degraded as well as endogenous DAF-7 would be. Combined with the report that *daf-7* is not expressed in *daf-11* mutants (89) and our previous observation that *egl-4(gf)* suppresses the quiescence defect of *daf-7* worms (20), this places cGMP both upstream and downstream of *daf-7* in satiety quiescence signaling. Since *daf-1* fat storage, feeding, and reproductive phenotypes are rescued by restoring the gene in the RIM and RIC interneurons (94), we also tested this rescue in satiety quiescence and found that it rescues this phenotype as well by both hand-eye and TOBO (Figure 14 and ref. 46). Additionally, laser ablation of the RIM and RIC interneurons rescues satiety quiescence in *daf-1* worms (46), suggesting that RIM and RIC are suppressing satiety quiescence, presumably by synthesizing a hunger signal. These neurons are the source of octopamine synthesis, which has previously been shown to decrease pumping rates (95,96). Additionally, *daf-7* has recently been shown to act as an environmental sensor signaling to RIM and RIC to inhibit tyraminerpic and octopaminergic neurotransmissions (94). We therefore tested whether exogenous octopamine would suppress satiety quiescence but found that it did not show an effect (46).

Figure 13

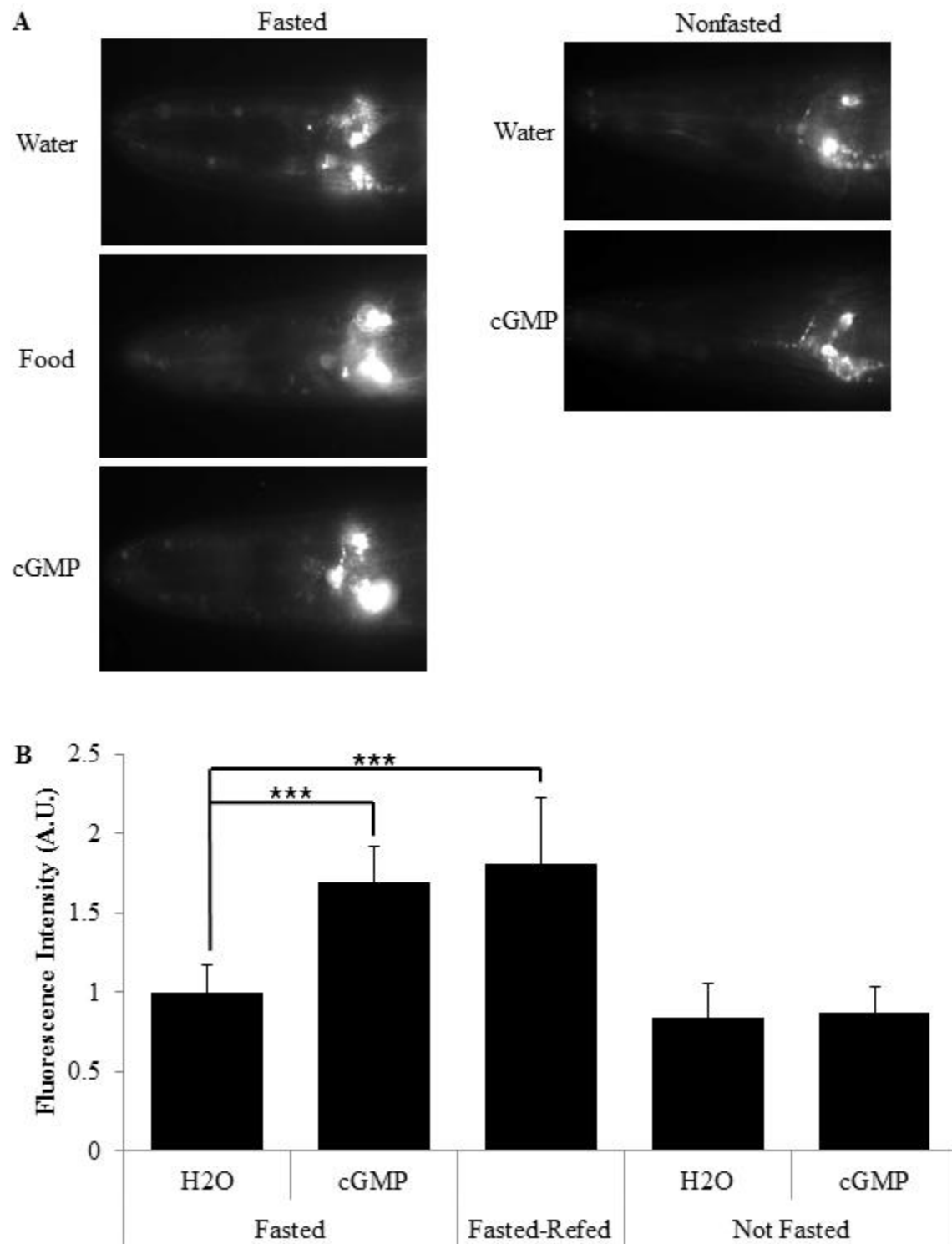


Figure 13. Food and cGMP increase levels of the TGF β ligand in fasted worms.

A. Representative images of worms expressing *daf-7p::daf-7::mCherry*. Left: Worms were fasted for 12 hours and either mock refeed for 3 hours on water treated NGMSR plates, NGMSR plates treated to final concentration of 1 mM 8-Br-cGMP for 3 hours, or refeed on HB101 for 3 hours. Right: Well-fed worms were placed on NGMSR water treated plates for 3 hours or NGMSR plates treated to 1 mM final concentration of 8-Br-cGMP for 3 hours.

B. Quantification of fluorescence intensity for conditions described in **A**.

*** $p < .001$ by Student's t-test.

Figure 14

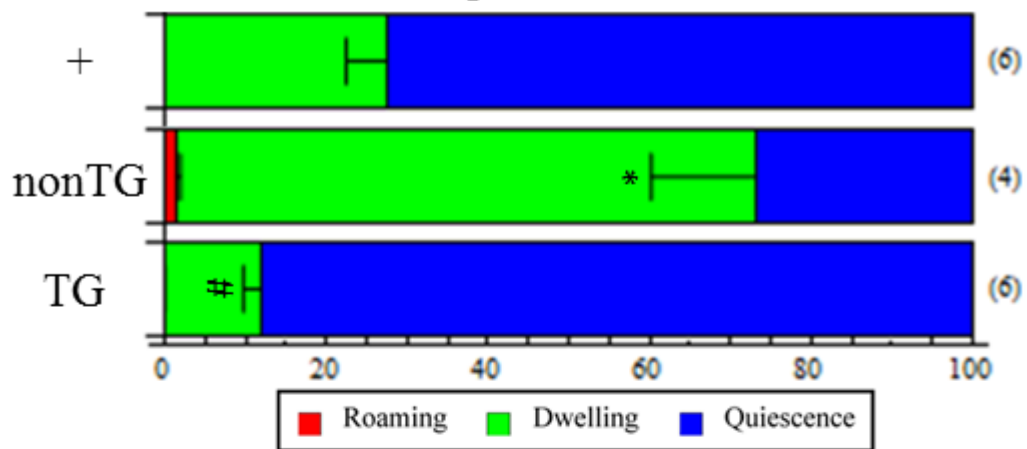


Figure 14. Restoring the TGF β receptor DAF-1 in RIM and RIC rescues satiety quiescence in *daf-1* worms after fasting and refeeding.

Wild-type worms were tested concurrently with matched transgenic (expressing *daf-1* in RIM and RIC under the *tdc-1* promoter) and nontransgenic siblings.

Number of tracks analyzed for each condition shown to the right of the data. Percent time in each behavioral state was determined by Pure Play Analysis. Experiments were done concurrently using TOBO.

* $p < 0.05$, compared to wild-type not treated, # $p < .05$ compared to nontransgenic Mann-Whitney U -test.

Together, this suggests that *daf-7* is released from ASI and binds to the *daf-1* receptor on RIM and RIC. This inactivates these neurons, causing an inhibition of hunger signaling and conveying quiescence. While octopamine is one of these hunger signals, it does not appear to be the satiety quiescence signal. Additionally, we know that *egl-4* is signaling downstream of *daf-7* but we do not yet know which cell(s) are responsible for this.

2.7 *egl-4* signaling in satiety quiescence

Exogenous 8-Br-cGMP both enhances quiescence in nonfasted worms and rescues the quiescence defect of *daf-11* guanylyl cyclase mutants (46). Additionally, expressing *daf-11* in the ASI neuron is sufficient to rescue its satiety quiescence defect (46). Our lab had previously found that the quiescence defect of *egl-4* worms (cGMP-dependent protein kinase) is rescued by restoring *egl-4* expression under the *tax-4* promoter (expressed in a dozen head neurons, including ASI (38)) (20). Our locomotion tracking and HMM analysis repeated this result. Restoring *egl-4* under its own promoter or the *tax-4* promoter rescued percent time in quiescence (Figure 15). Since *egl-4* is downstream of *daf-7* in satiety signaling and *daf-7* is expressed in ASI, we also tested whether expressing *egl-4* in ASI under the *gpa-4* promoter (97) rescues *egl-4(lf)* worms. We found that this gives a partial rescue, clearly enhanced from *egl-4(lf)*, but not as well as either the *tax-4* or endogenous promoter (Figure 15). We additionally tried to phenocopy the *egl-4(gf)* with transgenic expression of a constitutively active EGL-4 expressed under the *tax-4* promoter. This

Figure 15

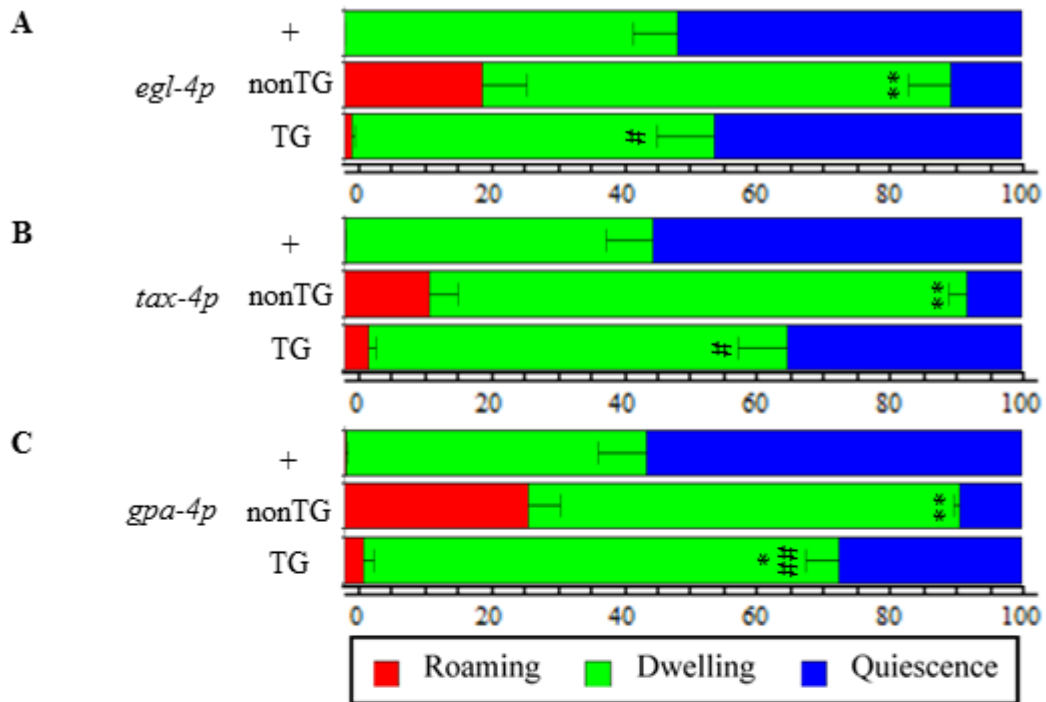


Figure 15. Restoring *egl-4* expression rescues satiety quiescence.

Wild-type worms were tested concurrently with matched transgenic (expressing *egl-4* under the indicated promoter) and nontransgenic siblings.

Standard state probabilities of worms which were concurrently assayed with wild-type worms using TOBO.

A. Restoring *egl-4* under the endogenous promoter rescues quiescence back to wild-type levels.

B. Restoring *egl-4* under the *tax-4* promoter (expressed in a dozen head neurons including ASI, (38)) rescues quiescence.

C. Restoring *egl-4* in ASI under the *gpa-4* promoter (97) partially rescues quiescence.

* $p < 0.05$, ** $p < 0.01$ compared to wild-type, # $p < .01$, ## $p < .01$ compared to non-transgenic by Mann-Whitney *U*-test.

resulted in significantly smaller body size (Figure 16A, B). To our surprise, this suppressed roaming but did not enhance satiety quiescence in nonfasted worms (Figure 16D). It did, however, enhance satiety quiescence after fasting and refeeding (Figure 16E).

While *egl-4* worms are impaired in satiety quiescence, they still respond to food quality and feeding history, two factors that are necessary for satiety quiescence. After fasting and refeeding, they show noticeably higher speed on poor quality food (Figure 17 A, B). Looking at average speed, *egl-4* worms showed increased locomotion both fasted-refed and nonfasted on poor quality food and after fasting and refeeding on high quality food (Figure 17C). This indicates that there are other factors that convey hunger and nutrition signals independent from satiety signaling that are still functioning in the *egl-4(lf)* worm.

2.8 ASI is activated by nutrition

Under adverse conditions, *C. elegans* larvae can enter a developmental diapause known as the dauer larvae (82). Food (79), ASI (83), and DAF-7 (50) inhibit dauer formation. These facts, combined with our results, previously described effects on behavior (20,39), and the proximity of metabolic signaling genes *egl-4* and *daf-7* suggested that ASI might respond to the worm's nutritional state to regulate satiety. We tested this prediction by calcium imaging. Calcium imaging uses a chimeric construct of GFP fused to calmodulin, which can be transgenically expressed in the cell of interest, in our case the

Figure 16

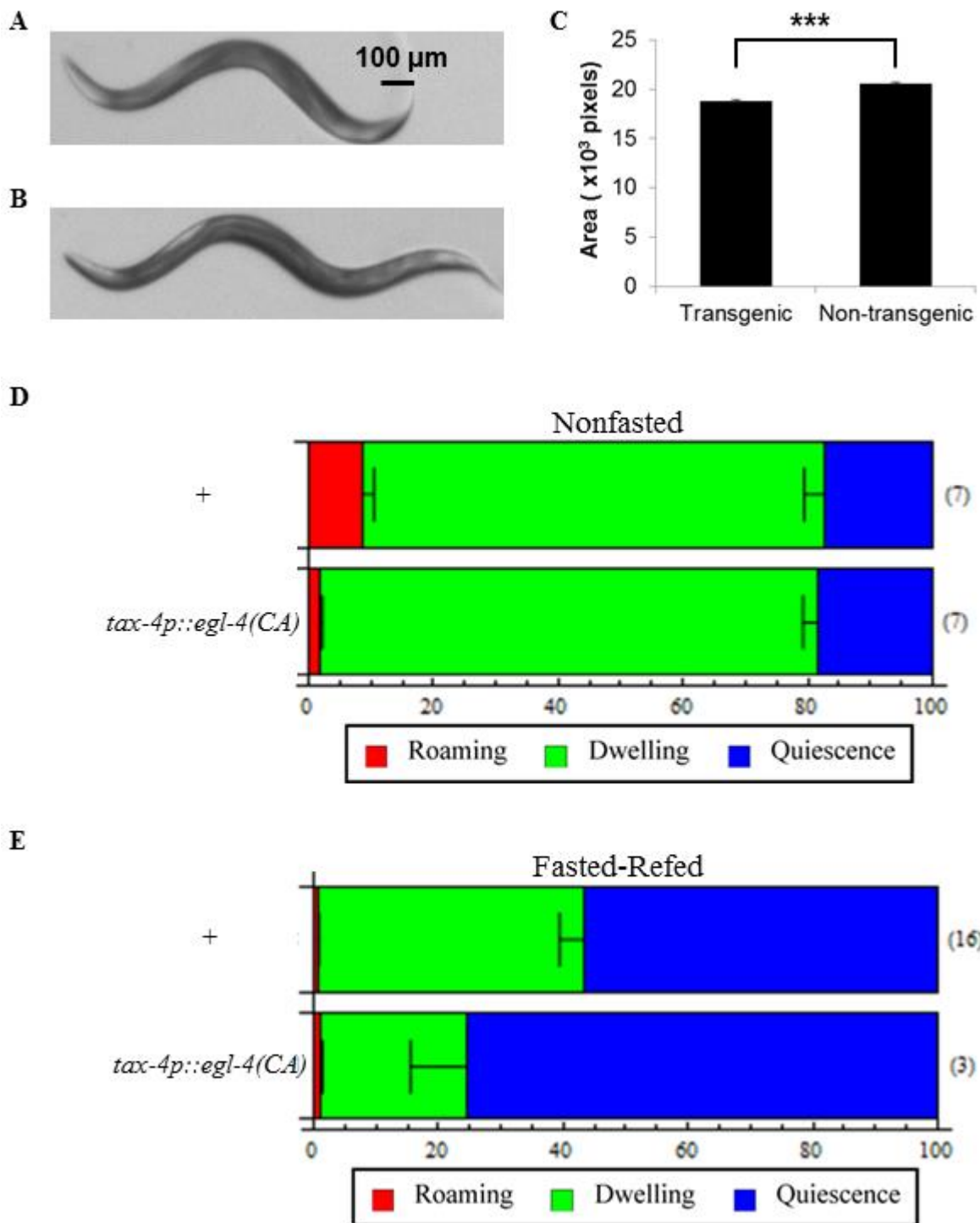


Figure 16. EGL-4 function for quiescence

Worms expressing EGL-4CA in TAX-4 neurons have smaller body size and more quiescence than their non-transgenic siblings after fasting and refeeding, phenocopying *egl-4(gf)*, as quantified by standard state probabilities.

A. Representative picture of an adult transgenic worm.

B. Representative picture of an adult nontransgenic worm.

C. Quantification of body size by area. *** $p < 0.001$, by Student's t test.

D, E. Quiescence is enhanced in fasted-refed transgenic worms but not in nonfasted transgenic worms. Number of tracks analyzed shown to the right of the data. Mann-Whitney U-test of percent time in quiescence for fasted-refed worms $p = .104$.

Data was collected before implementing TOBO and so was not done concurrently. Wild-type fasted-refed and nonfasted data is repeated from Figure 9.

Figure 17

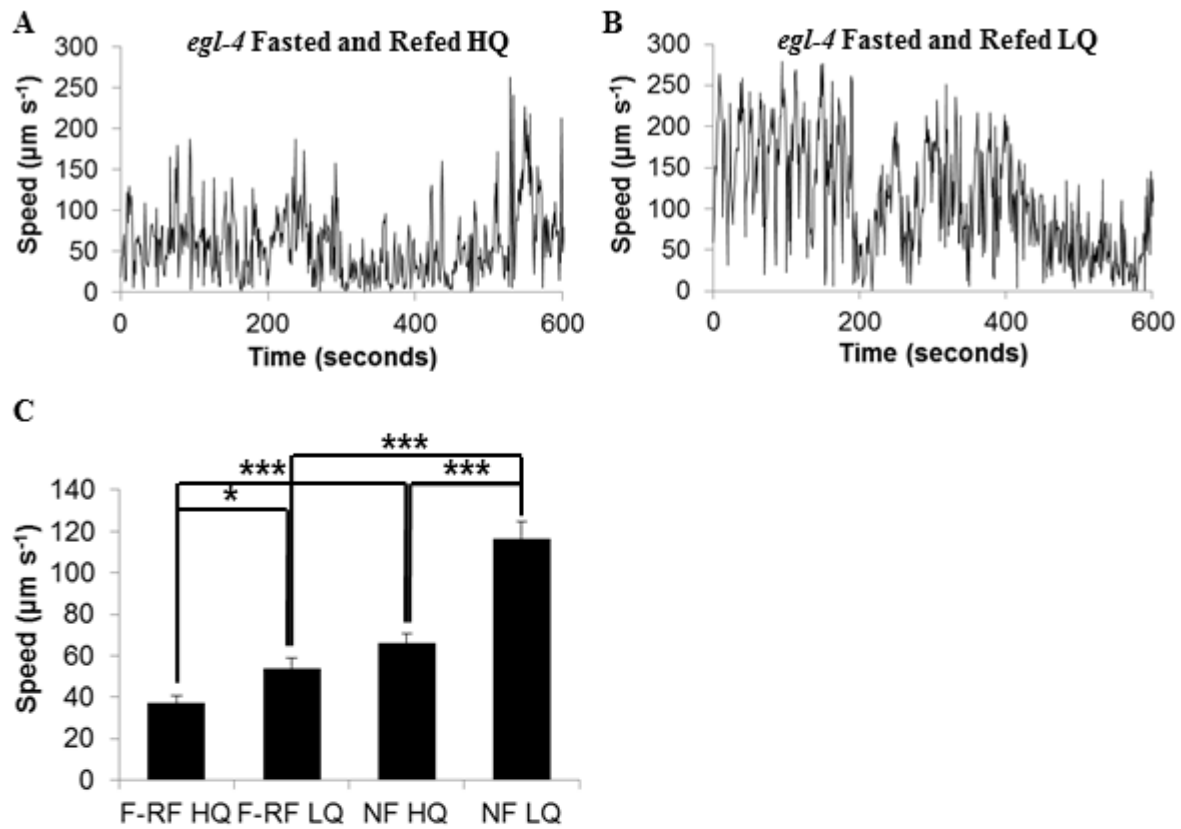


Figure 17. *egl-4* worms respond to nutritional state and food quality.

A. A representative speed plot of a fasted and refed *egl-4* mutant worm on high quality food.

B. A representative speed plot of a fasted and refed *egl-4* mutant worm on low quality food.

C. The mean speeds of *egl-4* mutants under different conditions: F-RF HQ: fasted and refed high quality food, NF HQ: non-fasted and fed high quality food. F-RF LQ: fasted and refed low quality food. Fasted and refed high quality food of *egl-4(lf)* was duplicated from Figure 1. Following Kruskal-Wallis ANOVA ($P < 0.001$), $*p < 0.05$. $***p < 0.001$, by Mann-Whitney *U*-test.

ASI neuron (98) and the ‘olfactory chip’ to flow a stimulus across the nose of the worm (99). Worms stimulated with either bacteria grown in minimal media or the nutrient rich solution Luria Broth (LB) showed a clear activation of the ASI neuron (Figure 18A, B). Stimulating worms with either minimal media alone or washed bacteria did not show activation of the ASI neuron (Figure 18C and data not shown). Since cGMP is signaling in ASI to promote satiety quiescence and ASI responds to the nutritional content of worms’ environment, we also tested whether cGMP can activate ASI. We found that ASI is activated by 1 mM of the stable analog 8-Br-cGMP but that this activation is weaker and less consistent than the response to food or LB (Figure 18D).

2.9 Additional satiety signaling

While our main interest has been further investigating the TGF β -cGMP pathway that is conveying satiety signaling, we have tested additional candidates hypothesized to play a role in satiety quiescence by our group and collaborators. One signaling group of particular interest is endocannabinoid signaling. Endocannabinoids are well known to play a role in gut-brain signaling and regulation of food intake (100–103). Importantly, a form of endocannabinoid signaling, N-acyl ethanolamines (NAEs), has recently been discovered in *C. elegans* playing a role in metabolic regulation, specifically in the dauer decision (104).

Figure 18

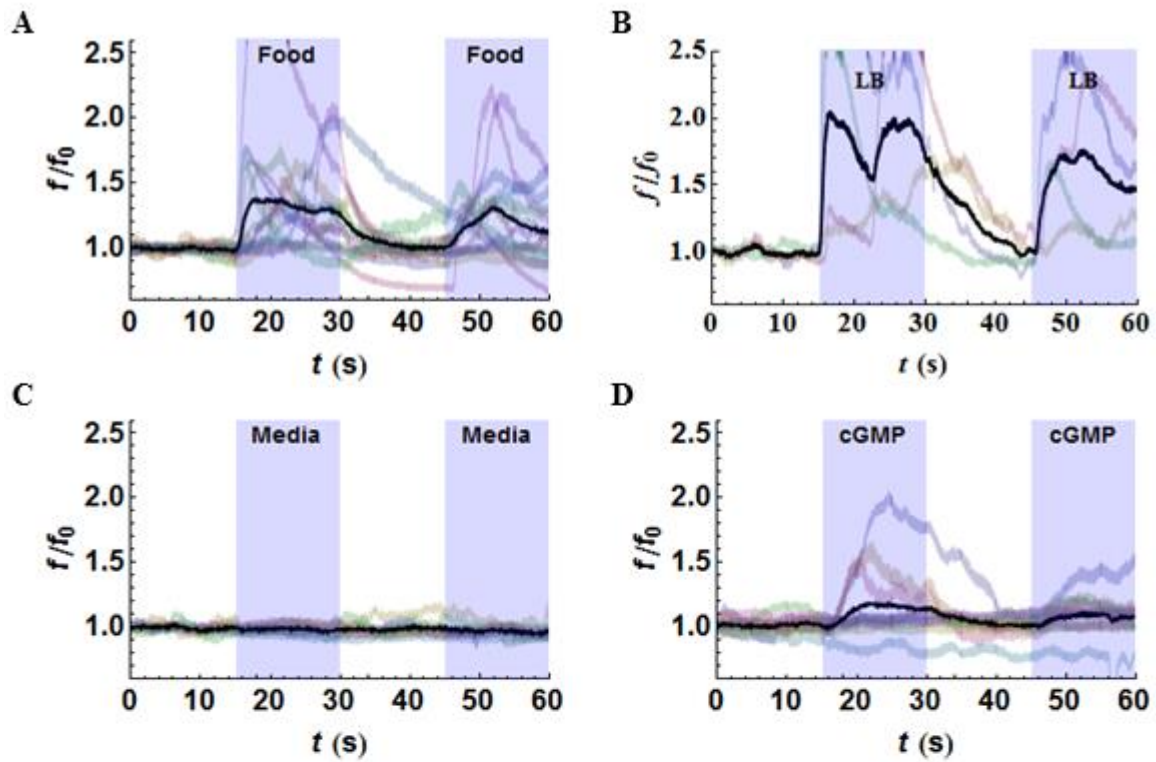


Figure 18. ASI responds to nutrition.

F-G. Ca^{2+} imaging from ASI neurons. GCaMP2.2 was expressed in ASI under the *gpa-4* promoter (97). One or both ASIs were imaged as either M9 buffer or an experimental stimulus flowed past the tip of the head, where the ASI sensory endings are located. The stimulus was presented from 15–30 seconds and again from 45–60 seconds. Individual traces, normalized so that the mean for the first 15 seconds (before presentation of stimulus) is 1, are shown in color (f is fluorescence, f_0 baseline fluorescence; the ratio is f/f_0). The dark black line is the mean of the normalized traces.

- A.** Worms stimulated with HB101 strain *E. coli* grown in minimal media.
- B.** Worms stimulated with Luria Broth.
- C.** Worms stimulated with minimal media alone.
- D.** Worms stimulated with 1 mM 8-Br-cGMP.

While a homolog of the cannabinoid-1 (CB1) receptor has not been found in worms, its inhibitor AM251 has metabolic effects in worms (Dr. Matthew Gill, personal communication). We tested whether AM251 either enhances satiety quiescence under conditions where worms spend little time in quiescence or whether it suppresses quiescence under conditions where it is enhanced. We found that in both the nonfasted and fasted-refed conditions there was little effect on time the worm spends in quiescence, but that treatment with the inhibitor caused worms to spend more time roaming at the expense of dwelling (Figure 19A, B). NAEs are synthesized by N-acyl-phosphatidylethanolamine-specific phospholipase D and degraded by fatty acid amide hydrolase, of which *C. elegans* have two and six genes respectively (104). Since no loss-of-function mutations of the synthesis enzymes have been isolated, we tested transgenic worms over expressing each one and both together. We also tested these overexpressers in the background of *faah-1* mutation, one of the enzymes that degrade NAEs. However we saw no impairment of satiety quiescence after fasting and refeeding or enhancement of quiescence in nonfasted worms (Figure 20A, B). This does not completely rule out NAEs playing a role in quiescence. There may be redundant function with the other five fatty acid amide hydrolase enzymes and NAEs are highest at the L2 stage and so we might not see as strong of a phenotype in mutant and transgenic worms at the adult stage.

Another group of signaling genes that were of particular interest is neuropeptides. Neuropeptides play a clear role in feeding behavior and worms that lack neuropeptide signaling are quiescence defective (20). We tested worms with feeding impaired ability to feed, *eat-1* and *eat-2* mutants. Both have been reported to have feeding defects and the

Figure 19

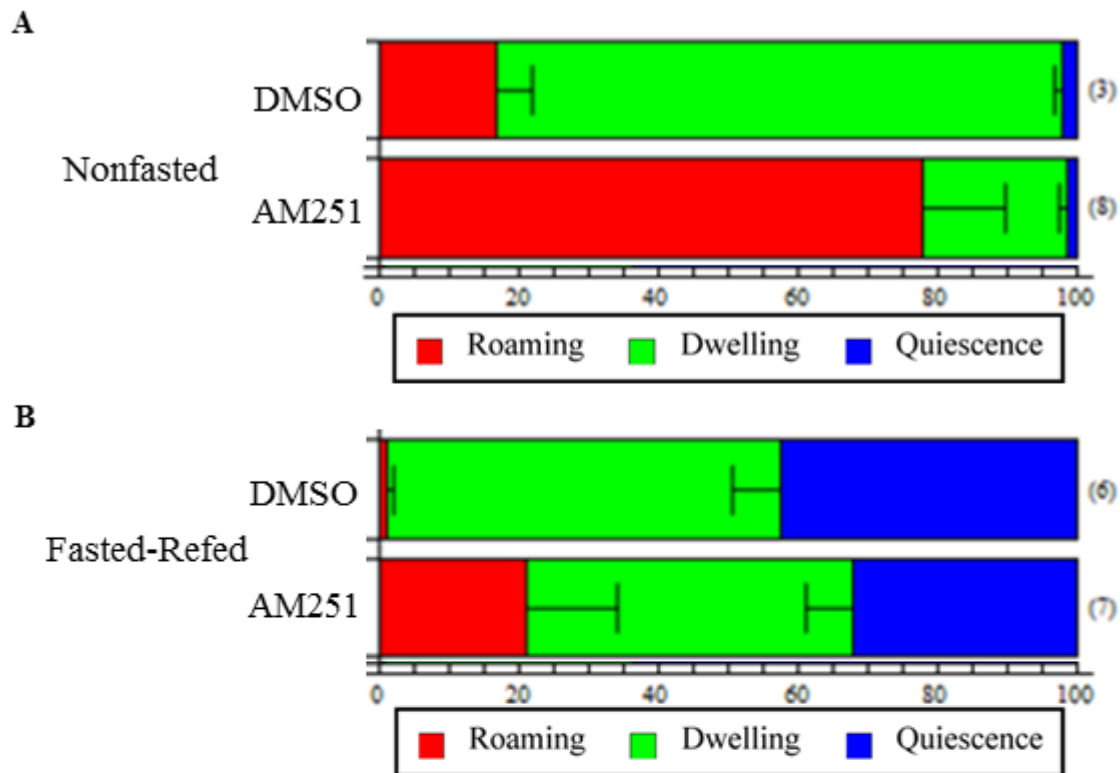


Figure 19. CB1 receptor inhibitor treatment increases roaming behavior.

Worms were treated for 3 hours on plates treated with either DMSO or the cannabinoid 1 receptor inhibitor AM251 (5 μ M). Number of tracks analyzed for each condition shown to the right of the data. Standard state probabilities of worms which were concurrently assayed with wild-type worms using TOBO.

A, B. Both nonfasted and fasted-refed worms treated with AM251 show enhanced roaming but no significant change in quiescence.

Figure 20

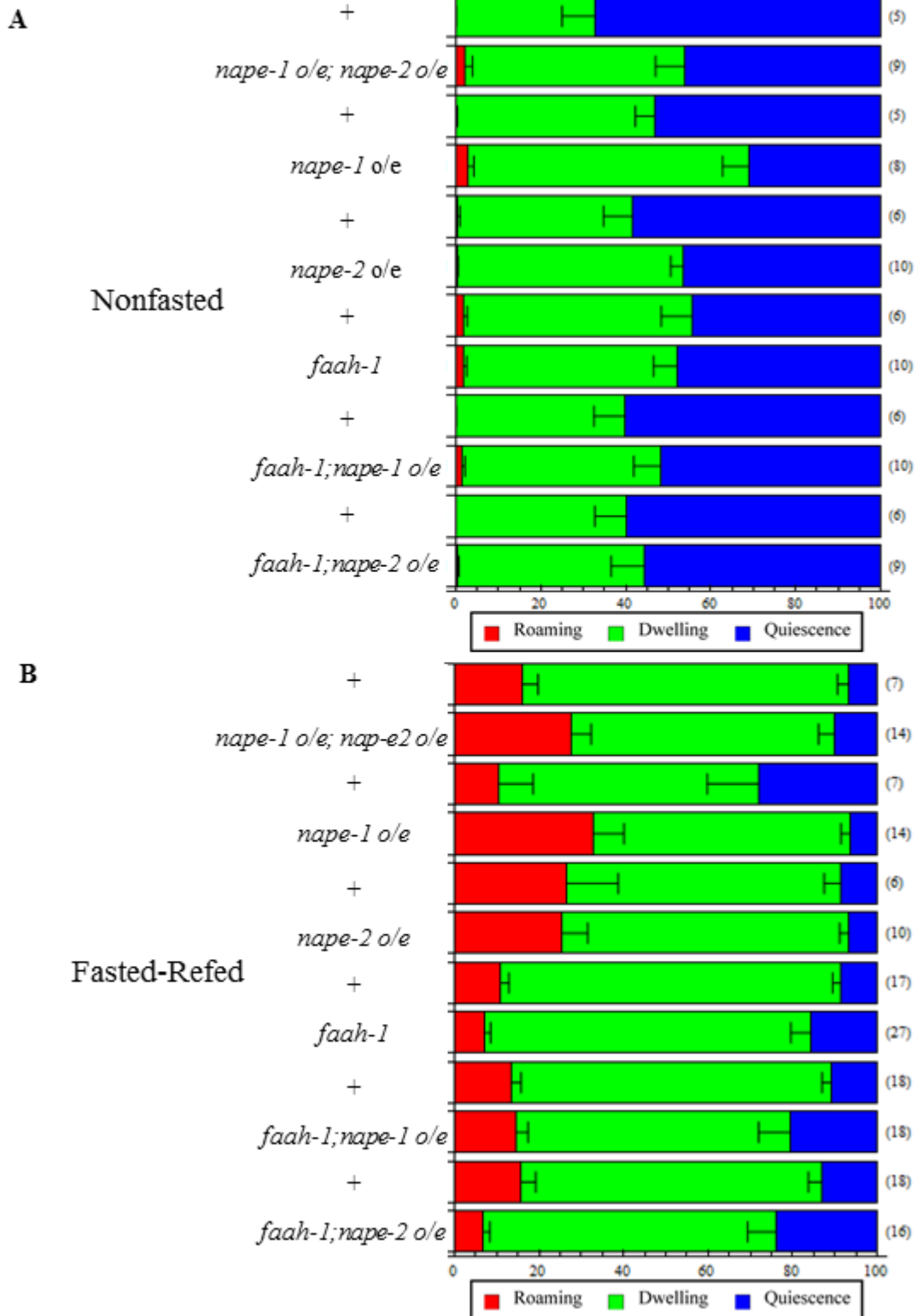


Figure 19. Endocannabinoid signaling regulation of satiety quiescence

Worms overexpressing the NAE synthesis enzymes *nape-1*, *nape-2* or both were tested for quiescence. Worms with a mutation in one of the enzymes that degrades NAEs, *faah-1*, were also tested. The overexpressing strains were also tested in the mutant background. Number of tracks analyzed for each condition shown to the right of the data. Standard state probabilities of worms which were concurrently assayed with wild-type worms using TOBO.

A. In the well-fed condition worms overexpressing either *nape-1*, *nape-2*, or both did not show a change in satiety quiescence levels. Expressing either *nape-1* or *nape-2* in the *faah-1* background likewise did not change satiety quiescence levels.

B. After fasting and full refeeding worms overexpressing either *nape-1*, *nape-2*, or both did not show a change in satiety quiescence levels. Expressing either *nape-1* or *nape-2* in the *faah-1* background likewise did not change satiety quiescence levels.

latter of which our group had previously reported to be quiescence defective (20,105–107). We found that *eat-2* worms have decreased quiescence and increased roaming in both nonfasted and fasted-refed conditions (Figure 21A, B). As we expected, *eat-1* worms show a similar decrease in satiety quiescence after fasting and refeeding (Figure 21B). Curiously, however, nonfasted *eat-1* worms show an increase in both quiescence and roaming (Figure 21A).

Our lab had previously done a microarray analysis to find genes whose expression changed with fasting and after refeeding. We tested a selection of neuropeptide mutants that had shown significant changes in expression, *nlp-2*, *nlp-22*, *ins-7*, and *ins-33*. However, after fasting and refeeding we saw no significant differences in satiety quiescence in any of these mutants (Figure 22).

Along with neuropeptides, we are interested in ways that neurons can be communicating satiety signaling. Multidrug resistance proteins (MRPs) transport molecules through the cell membrane and are highly conserved between worms and humans with homologs of all eight families of MRPs (108). We hypothesized that MRPs might transport molecules such as cGMP either into or out of cells which will then affect satiety signaling. Interestingly, we found that *mrp-2* mutant worms showed higher levels of quiescence than wild-type worms in the nonfasted condition (Figure 23A, B).

We also investigated a signaling pathway downstream of *daf-7*, *glr-1*. GLR-1 is an ionotropic glutamate receptor that has previously been shown to play a role in neuronal control of locomotion (109) that has previously been studied in regulating *daf-7* phenotypes (94). However, we saw no change in behavioral state in either *glr-1* worms

compared to wild-type or in *daf-7 glr-1* worms compared to *daf-7* worms both fasted and refed as well as nonfasted (Figure 24A, B).

Figure 21

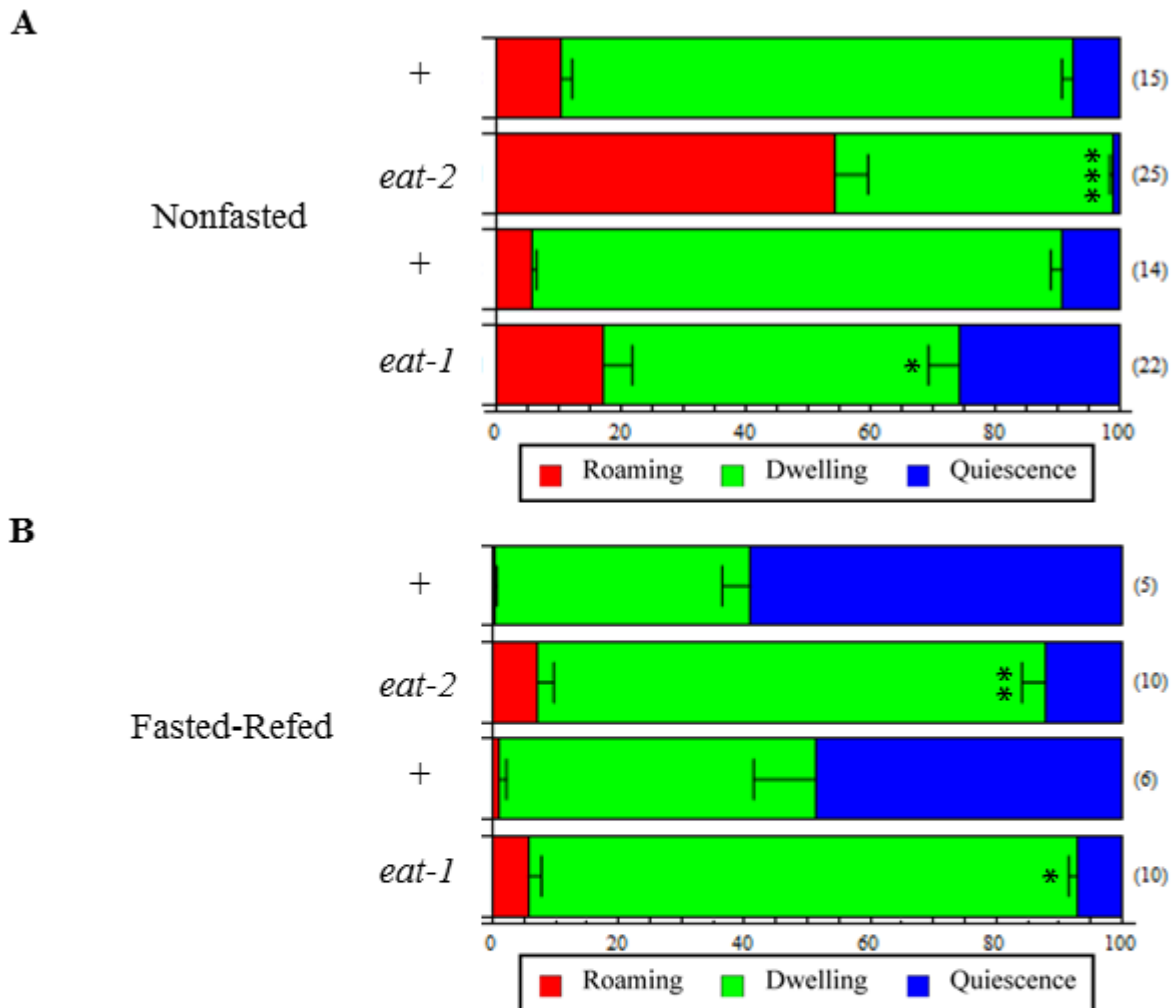


Figure 21. Worms with feeding defects show altered quiescence behavior.

eat-1 and *eat-2* mutants were tested both nonfasted and after fasting and full refeeding. We previously reported that *eat-2* worms be quiescence defective after fasting and refeeding (20). Number of tracks analyzed for each condition shown to the right of the data. Standard state probabilities of worms which were concurrently assayed with wild-type worms using TOBO.

A. Nonfasted *eat-2* worms show less quiescence and more roaming as we had expected.

Curiously, *eat-1* worms showed both increased roaming and quiescence.

B. After fasting and refeeding both *eat-1* and *eat-2* worms both show more roaming and less quiescence.

* $p < 0.05$, ** $p < 0.01$, *** $p < 0.001$ compared to wild-type by Mann-Whitney *U*-test.

Figure 22

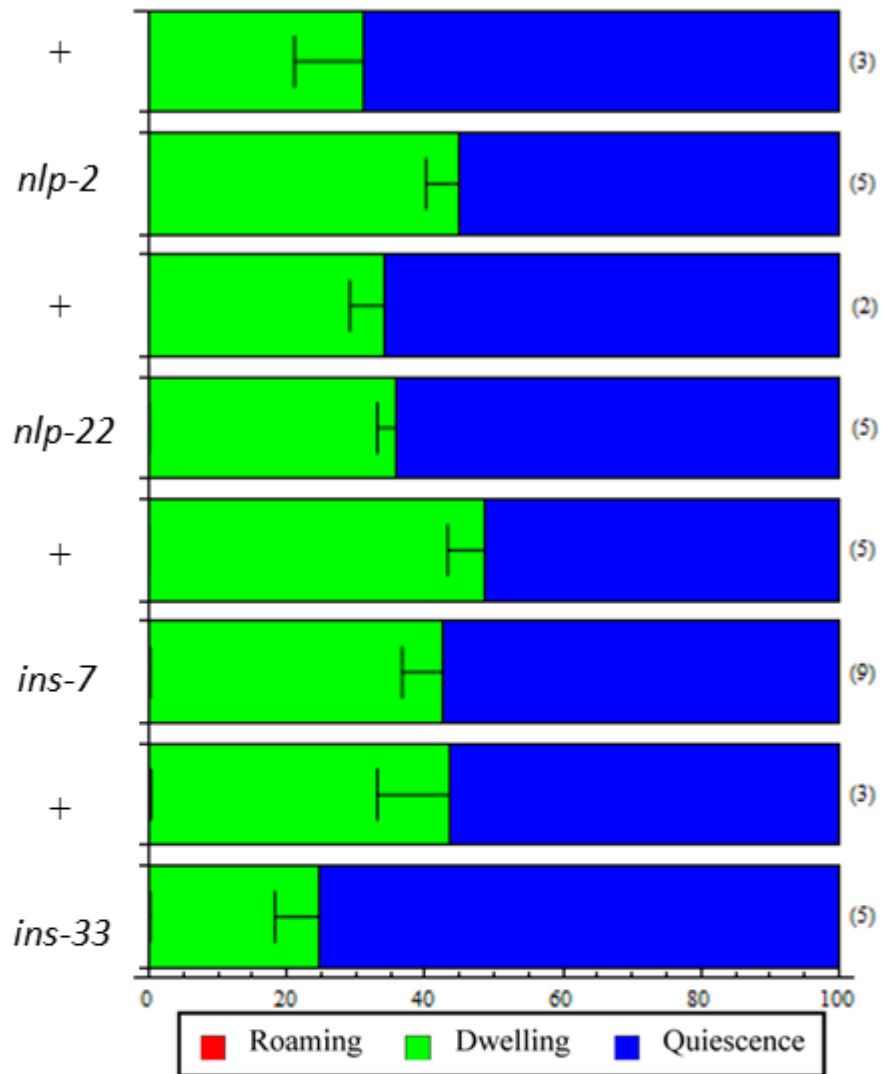


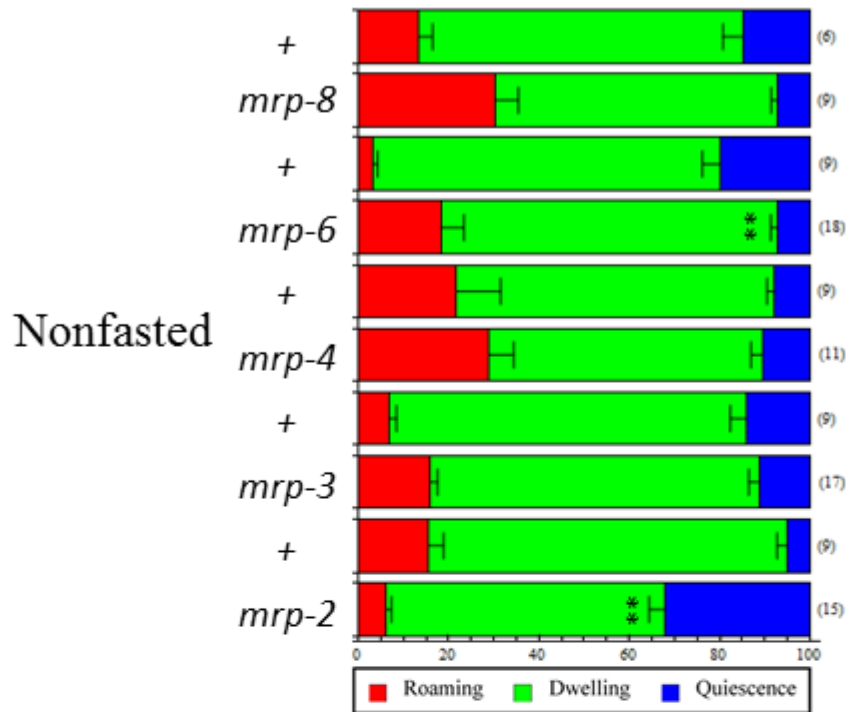
Figure 22. Selected neuropeptide mutants show no change in quiescence.

Number of tracks analyzed for each condition shown to the right of the data. Standard state probabilities of worms which were concurrently assayed with wild-type worms using TOBO.

A, B. *nlp-2*, *nlp-22*, *ins-7*, and *ins-33* mutant worms show no significant difference in percent time quiescent either nonfasted or after fasting and refeeding.

Figure 23

A



B

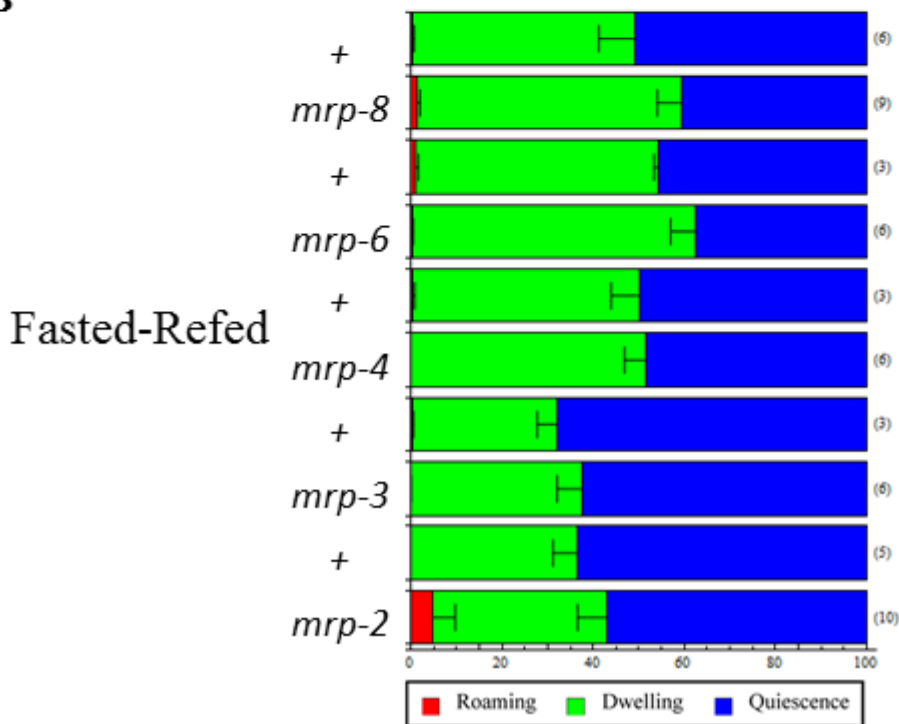


Figure 23. Multidrug resistant protein genes may play a role in conveying satiety signals.

Number of tracks analyzed for each condition shown to the right of the data. Standard state probabilities of worms which were concurrently assayed with wild-type worms using TOBO.

A. Nonfasted *mrp-2* worms show increased satiety quiescence and *mrp-6* worms show decreased satiety quiescence while *mrp-3*, *mrp-4*, and *mrp-8* show no change in satiety quiescence.

B. None of the worms with mutations in MRP genes showed a significant change in satiety quiescence after fasting and refeeding.

** $p < 0.01$ compared to wild-type by Mann-Whitney *U*-test.

Figure 24

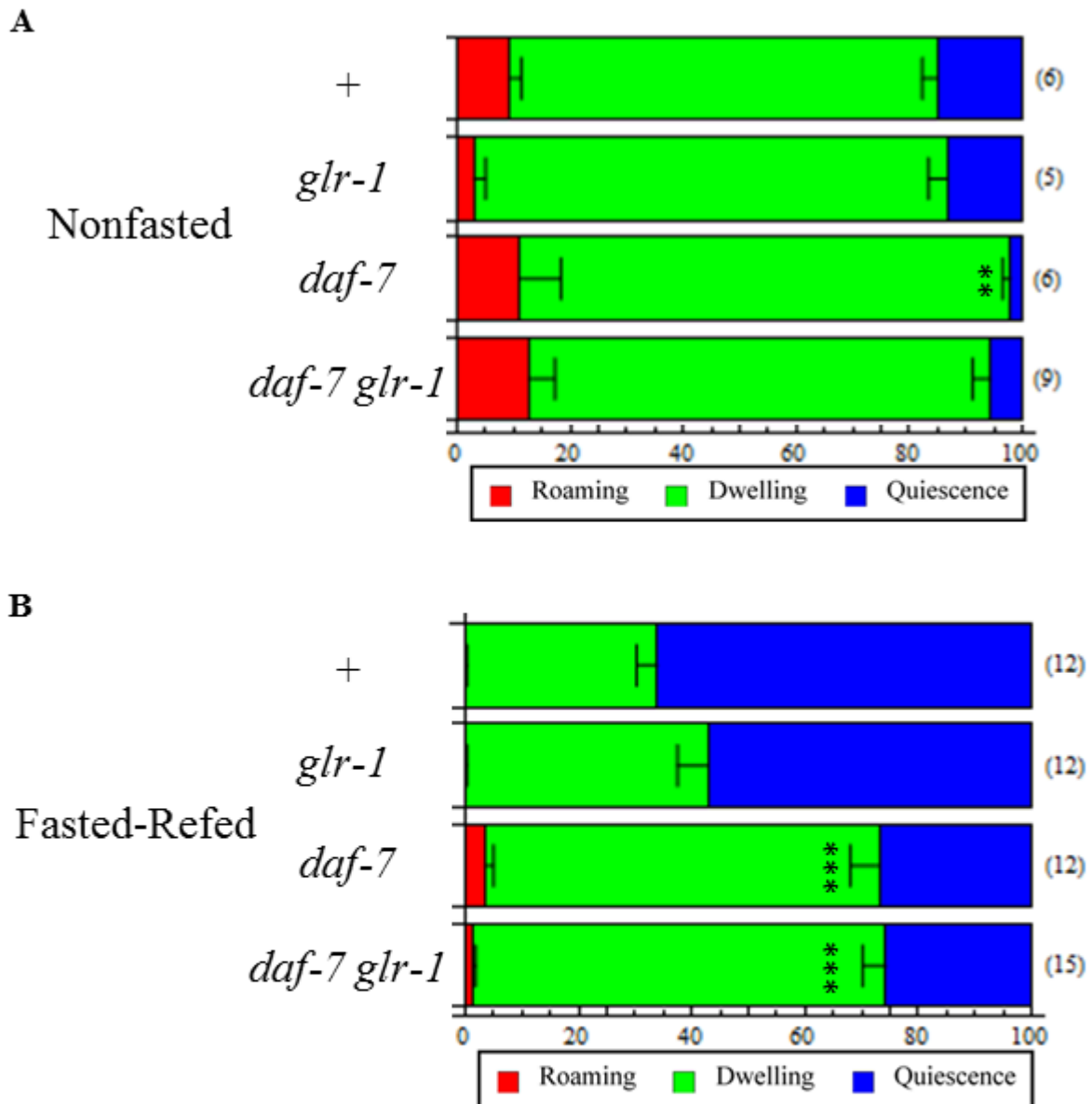


Figure 23. *glr-1* has no effect on quiescence.

A. Nonfasted *glr-1* worms show no significant change in behavior either in the wild-type background or in the *daf-7* background.

B. Nonfasted *glr-1* worms show no significant change in behavior either in the wild-type background or in the *daf-7* background.

Number of tracks analyzed for each condition shown to the right of the data. Standard state probabilities of worms which were concurrently assayed with wild-type worms using TOBO.

** $p < 0.01$, *** $p < 0.001$ compared to wild-type by Mann-Whitney U -test.

3. Conclusions and future directions

Throughout human evolutionary history food has mostly been scarce. However, today we find ourselves in a novel environment where food is readily available and the energy required for day to day survival is minimal. This has caused a dramatic increase in the prevalence of obesity and its secondary health conditions, leading to decreased life quality and span as well as placing a significant burden on the healthcare system. Part of the obesity epidemic can be attributed to overeating- consuming more calories than day to day activity requires, the excess of which is stored as fat. We have found a worm behavior that mimics aspects of post prandial sleep in mammals and are investigating the signaling that enhances and disturbs this behavior in an effort to better understand the interactions of the molecules we have discovered so far and to uncover more genes signaling to convey this behavior, which are likely to have evolutionarily conserved homologs playing similar roles in mammals.

Behavior is a result of neuronal wiring and cellular signaling that conveys a response to an animal's environment, nutritional state, and external stimuli. *C. elegans* have a comparatively simple neuronal wiring with only 302 neurons. We have worked to develop tools that allow better analysis of worm behavioral state so that we may better investigate the neuronal connectivity and signaling pathways that are responsible for the cessation of food intake. The work presented here combines this locomotion tracking and HMM analysis with additional genetic and cell biology approaches to better understand satiety signaling.

Satiety quiescence is the complete cessation of locomotion and feeding. Why is this advantageous? Evolutionarily, why would this behavior arise? Would worms in satiety quiescence be more vulnerable to predators and consume less food? In beginning to address these questions about worms, we can first ask them about ourselves. If food is so critical to our survival, why do we have mechanisms that tell us to stop eating? Why do we go into a resting and fasting state that makes us more vulnerable to predation? Two answers come to mind to answer these questions.

First, satiety quiescence could be a means of maximizing the efficiency of using the resources available. This coincides with a switch from a state of energy stress when the worm was depleting its stored energy to storing energy and producing progeny. The intestine of the worm experiences a pressure from the food in balanced with the waste out. When a worm is continuously feeding, the worm must continuously be expelling waste. If the worm stops feeding, it can more fully utilize the nutrients it has already taken in. Cessation of locomotion does expose an animal to increased risk of predation. However, this is not a comatose like state; worms are easily disturbed from quiescence and sensing a predator such as a larger nematode or mites would likely alter the behavior as a roar from a lion would alter the behavior of a human. Additionally, this risk is balanced by the benefit of maximizing its speed in having its offspring and laying those offspring on a high quality food source, which is essential for an animal whose reproductive strategy is to quickly have large numbers of progeny.

Second, while we do not know why we need sleep, it has been found to be important both metabolically and neurobiologically. Cessation of feeding and locomotion

in sleep or sleep-like behavior is a common phenomenon across many phyla. While worms lack the central nervous system required to define sleep, quiescence is at least very similar to mammalian sleep. Developmentally, worms become quiescent just before molting in a behavior that has been termed lethargus, which may be important in the metabolism of development. After feeding, mammals and birds go through a behavioral satiety sequence which ends with the animal sleeping.

An additional question to consider is what determines the basal level of quiescence? If this is a behavior to maximize the use of resources available, would high levels of quiescence be expected under normal growth conditions? One factor to consider is the need for dispersal. A worm growing in optimal conditions likely has hundreds to thousands of other worms growing along with it. Eventually the food source will run out and the evolutionary success of an animal is going to depend on the population's ability to disperse and find new food. Testing the ideas put forward here are challenging but intriguing. We assay worms one per plate, but these ideas would predict that conditioning plates with media from high numbers of *C. elegans* would suppress quiescence in nonfasted worms. Additionally, we would predict that refeeding worms on plates conditioned with media from a predatory nematode such as *Pristionchus pacificus* should disturb worm behavior. On the other hand, these ideas predict that placing a single egg on a plate and allowing a worm to grow in isolation should enhance quiescence as a worm tries to maximize its growth rate to produce progeny more quickly. This would also predict that if a worm is uncertain about its nutritional environment, it should attempt to increase its efficiency and so enhance quiescence. We have plans to test this idea by using worms

that have experienced starvation at various points in its development and assay satiety quiescence both fasted-refed as well as nonfasted.

Since our group's discovery of the satiety quiescence behavioral state, further investigation into the signaling that controls it has been difficult because the worms are easily disturbed from it under observation and the assay provides information limited to whether the worm is in quiescence when observed and if so what the duration of quiescence is. We have attempted to overcome these challenges by developing an automated system to record and track worms over long periods of time. Our locomotion tracking system finds distinct periods of inactivity that are consistent with satiety quiescence behavior. To quantify behavior over time we have used a Hidden Markov model analysis. We expected that this would find clusters of worm behavior corresponding to roaming, dwelling, and quiescence in state-space. However, while it appears that there are times where worms placed in specific conditions show "pure" behavioral state (i.e. straight high speed movement in roaming, short back and forth movements in dwelling, and completely unmoving in quiescence), over the timecourse of our recordings of numerous conditions and genotypes there is no clear grouping of clusters corresponding to these behavioral states. Instead, worm behavior appears to form a continuum in state-space. This suggests that worms are able to modulate their behavior more than simple switches between inactive, browsing, and exploratory modes.

While it is a simplification of worm behavior, we are able to assign behavioral states on a probabilistic basis over time from the locomotion data. Although this automated system does not find satiety quiescence levels as high as when worms are measured by

hand and eye, as we had previously done, it is sufficiently robust to repeat findings made by hand and eye and extend these to allow us to move our investigation of satiety quiescence forward.

It has been shown that a cGMP pathway regulates locomotive activity related to nutritional status (20,38,42,69,110). Our new automated monitoring system confirmed that *egl-4* is absolutely required for satiety quiescence; we did not detect inactive locomotive periods in *egl-4* mutants. Increased function of EGL-4 in ASI by a gain of function mutation enhances satiety quiescence, suggesting *egl-4* function in ASI. However, *egl-4* is required in other cells than ASI because expressing *egl-4* only in ASI did not fully rescue the *egl-4* mutant defect in satiety quiescence. This suggests that there are action sites other than ASI for EGL-4 to regulate satiety quiescence. Interestingly, an *egl-4* mutant can still respond to the changes in nutritional status, such as difference in food quality. Because *egl-4* mutants are completely incapable of showing satiety, this ability suggests that the increase of locomotion by low food quality can be caused by another signal likely coming from hunger. Our low quality food in fact made worms appear starved. It is interesting to speculate that the whole range of locomotive activity can be controlled by the integration of two types of signals: one to sense fullness and the other to sense hunger.

We found that cGMP signals upstream of TGF β to increase the levels of the ligand DAF-7 in fasted worms. Treating fasted worms with 1 mM 8-Br-cGMP increases DAF-7 levels to a similar degree as refeeding worms on high quality food. This occurs in the ASI neuron, which we and others have shown to be a major center of integration of signals that convey the nutritional state of the worm. We have added to this the information that the

ASI neuron is activated by the nutritional content of the worm's environment, meaning that the ASI neuron is sensing both the internal and external nutritional state of the worm.

How ASI integrates this short term (almost instantaneous) activation with a more long term (on the order of three hours) genetic program is still unknown. Our calcium imaging studies were done on well-fed worms, but the worms are food deprived for the time that it takes to load them into the microfluidic device, which is about five minutes. Activation of ASI could play a role in telling the worm to remain on food by starting to synthesize and/or release signals conveying that it is in a good environment. One such signal is cGMP. We plan to test the hypothesis that food stimulates an increase in cGMP levels in several ways. First, we will directly test whether cGMP levels increase using a cGMP reporter construct similar to GCaMP (60). This will tell us whether stimulation with food causes a change in cGMP levels on the same timescale as the calcium transient that we see. If we do see an increase, we will test both calcium and cGMP levels of worms with each *tax-4* and *daf-11* mutations. *tax-4* forms a heterodimer with *tax-2* to make a cGMP gated cation channel. *daf-11* is a membrane bound guanylyl cyclase. We are unable to test *tax-4* mutants for satiety quiescence because the worms do not stay on food and so we cannot observe them. *daf-11* mutants have deficient satiety quiescence, but are rescued by expressing the gene in the ASI neuron. Loss of cGMP or calcium transient in either the *daf-11* or *tax-4* background in response to stimulating the worm with food would suggest activation of *daf-11* → increased cGMP levels → activation of *tax-2/tax-4* channels as the pathway of how ASI is activated. Interestingly, this is the same pathway of activation proposed independently by a group studying the ASEL neuron mediating worm response

to pH levels, the only difference being that the guanylyl cyclase is *gcy-14* rather than *daf-11* (61). If our hypothesis holds, this suggests that this activation pathway could have developed evolutionarily specialized in individual worm neurons to respond to specific stimuli.

The question still remains of how ASI integrates this short term activation with long term induction of satiety quiescence. Looking into this question, there are two important pieces of information to consider. First, our studies of ASI activation simply looked at whether the neuron was activated acutely in response to a stimulus. What the neuron's pattern of activation looks like with continuous stimulation over time would be very valuable data to provide insight on its role in inducing quiescence. Second, satiety quiescence signaling must originate from the gut, meaning that activation of ASI is not sufficient for quiescence signaling. We can acquire information on the pattern of activation of ASI under continuous stimulation to provide more information on its signaling. Ideally this would be done in freely moving worms to correlate worm locomotion with neuronal activity. However, there are two technical challenges to accomplishing this. First, this approach would require a mechanical stage moving to keep the worm in a small field of view which is likely to disturb worm behavior. Second, continuous stimulation with fluorescent light disturbs worm behavior. This has been countered by using worms with loss of function *lite-1*, but this comes with additional caveats of the *lite-1* mutation possibly having an effect on worm behavior.

Upstream of the satiety quiescence signaling in ASI, we know that a signal that originates in the intestine is required. What this signal is and how it causes a response in

ASI we do not yet know. The fact that the signal originates in the intestine was established from the findings that worms that have pumping defects, and so are less able to intake food, and worms that have a microvillus-specific actin mutation, and so are less able to absorb nutrients, have deficient satiety quiescence. In mammals, much of the integration of appetite control between the intestine, liver, and adipose tissue is done by endocrine factors. Since worms lack major endocrine signaling molecules such as leptin, this might not be conveyed in the same way. We have several ideas and candidate approaches that could address what this signal might be. First, it could be transport of a secondary messenger such as cGMP across the intestine into the pseudocoelom, where it could reach the ASI neuron. We have attempted to address this by testing worms with mutations in multidrug resistant proteins. If we find genes that affect satiety quiescence, we will restore expression in the intestine and/or the ASI neuron to rescue quiescence to verify that this is where they are acting. It could be that nutrients, either a component of the bacteria or metabolized product, enters the pseudocoelom by diffusion through the intestine. If this is the case, a genetic approach would be difficult and a more biochemical approach would work better. Supplementing the NGM plate with various nutritional factors such as sugars, amino acids, or fatty acids would provide insight as to what triggers the communication from the intestine to ASI. Another interesting possibility comes from investigation into the innate immunity system. A recent report of communication between the intestine and nervous system in response to pathogenic bacteria implicated the insulin signaling system in canonical *daf-2* → *daf-16* signaling (111). While we have avoided the crowded insulin signaling field in favor of more novel signaling pathways, the fact that *daf-2* is upstream of

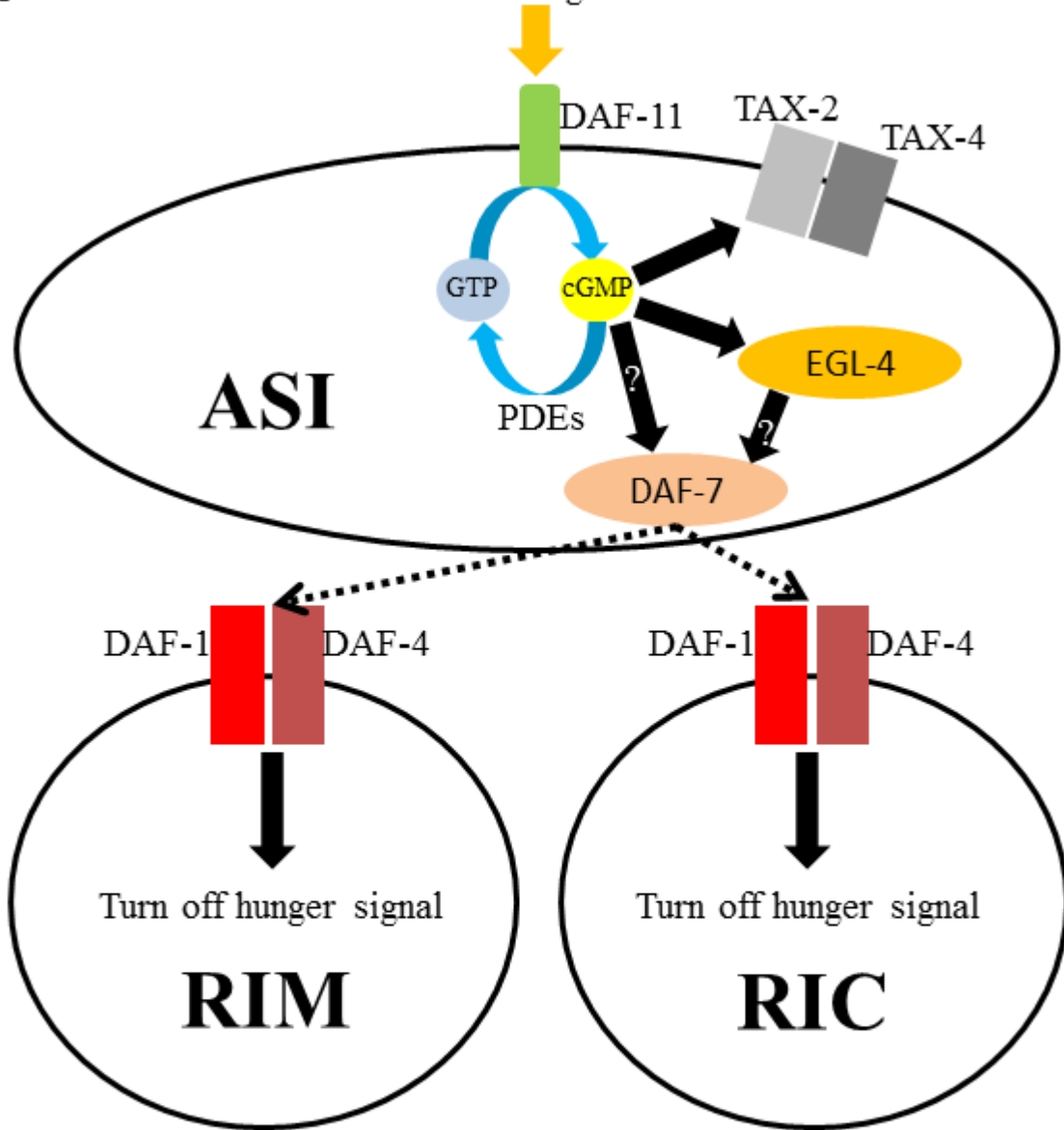
egl-4 in satiety signaling could be an indication that an insulin like peptide might be released from the intestine to communicate to ASI. In general, neuropeptides with reported expression in intestine are a great candidate pool to find what is initiating satiety signaling.

Downstream of ASI, we have shown that restoring the TGF β receptor *daf-1* in the RIM and RIC neurons rescues the quiescence defect of *daf-1* mutant worms. This means that cGMP is signaling to activate the canonical TGF β pathway, which connects ASI \rightarrow RIM + RIC. Ablation of these neurons in *daf-1* mutant worms rescues as well, pointing to *daf-7* \rightarrow *daf-1* signaling causing an inhibition of these neurons. We propose a model by which food signal activates ASI, causing *daf-11* to synthesize cGMP, which then activates EGL-4 and increases DAF-7 levels. DAF-7 is released from ASI and binds to its receptors DAF-1 and DAF-4 to inhibit synthesis of a hunger signal (Figure 25A). In terms of behavioral state, we propose that ASI promotes the switch from dwelling to quiescence and inhibits the switch from quiescence to dwelling. RIM and RIC do the opposite, promoting the switch from quiescence to dwelling and inhibiting the switch from dwelling to quiescence. This dynamic is modulated by the ability of ASI to suppress RIM and RIC activity via TGF β signaling (Figure 25B).

What specifically RIM and RIC are doing and what is downstream of these neurons we do not know. We hypothesized that octopamine, the invertebrate equivalent of noradrenaline which is synthesized in RIM and RIC, is the hunger signal but exogenous octopamine treatment did not suppress satiety quiescence. We plan to perform calcium imaging in these neurons to verify that their activity is suppressed under conditions where satiety quiescence is enhanced.

Figure 25
Food Signal

A



B

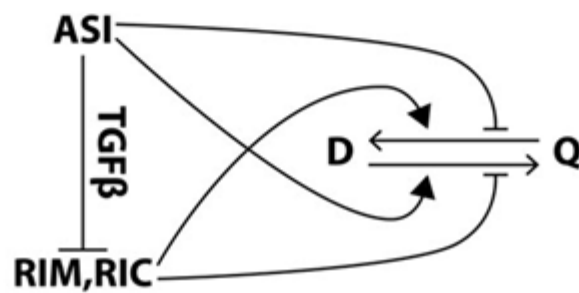


Figure 25. Proposed model of satiety quiescence signaling of cGMP and TGF β in

ASI \rightarrow RIM + RIC.

A. Signaling pathway. Food signal stimulates DAF-11 to increase cGMP levels in ASI, which then acts on its two known targets, the cyclic nucleotide gated channel formed by TAX-2 and TAX-4 and the cyclic GMP dependent protein kinase EGL-4. Downstream of cGMP, DAF-7 levels are increased and it is and released from ASI, where it binds to its receptors DAF-1 and DAF-4 on RIM and RIC. This inactivates a hunger signal synthesized by these neurons.

B. Behavioral dynamic. ASI promotes the switch from Dwelling to Quiescence and inhibits the switch from Quiescence to Dwelling. RIM and RIC does the opposite, promoting the switch from Quiescence to Dwelling and inhibiting the switch from Dwelling to Quiescence. ASI is able to modulate this dynamic by synthesizing and releasing the TGF β ligand DAF-7 to inactivate RIM and RIC.

In finding what is downstream of RIM and RIC, there are two approaches: what cell(s) they are communicating to and what molecule(s) are being used for this signal. For the first approach, a starting place is what synapses RIM and RIC form. Since the neuronal connectivity is known, this is a straightforward task to ablate these neurons and see whether satiety quiescence is enhanced. However, if the signal produced by RIM and RIC is released then these are not likely to be the target and the cell(s) that receive the signal would not be predictable from this information (just as the $ASI \rightarrow RIM + RIC$ connection is not predicted by neuronal connectivity). If this is the case, then returning to *egl-4* signaling is a possible route. We know that *egl-4* is signaling downstream of *daf-7* and so finding what cell(s) *egl-4* is acting in would reveal additional pieces of the satiety quiescence signaling puzzle. This could be accomplished by expressing constitutively active *egl-4* (*egl-4CA*) under neuron specific promoters in a *daf-7* or *daf-1* background. We would first have to verify that expressing *egl-4CA* in ASI does not enhance satiety quiescence, as our model predicts. First, we would express *egl-4CA* in RIM and RIC to answer the simple question of whether *egl-4* is acting on both sides of the *daf-7* $ASI \rightarrow daf-1$ RIM + RIC connection. If that is unsuccessful, we would target individual head neurons for *egl-4CA* expression. If this approach is successful, we will have identified a neuron downstream of RIM and RIC, allowing us to examine genes expressed in RIM and RIC that are likely to be released and have a receptor on the target cell. If this approach is unsuccessful, we can attempt a forward genetic screen. First, we would verify that the signaling in RIM and RIC is canonical TGF β with $daf-7 \rightarrow daf-1 \rightarrow daf-8 + daf-14 \dashv daf-3 + daf-5$. *daf-3* and *daf-5* repress gene transcription and mutants of *daf-3* and *daf-5* should

act as constitutively active *daf-1* and so should show either normal or enhanced satiety quiescence. A forward genetic screen in *daf-3* or *daf-5* mutants looking either specifically for satiety quiescence or indirectly for increased feeding and fat storage (*daf-3* and *daf-5* mutants rescue the increased feeding and fat storage of *daf-1* and *daf-7* worms) would identify genes downstream of the TGF β pathway, possibly identifying the hunger signal produced by RIM and RIC. We would expect that loss of function *egl-4* would cause this effect and so any hits isolated from this screen would need to be complementation tested with *egl-4*.

In addition to the cGMP-TGF β signaling axis, we have looked at a few other signaling pathways for potential effects on satiety quiescence. Some, such as *glr-1*, have no effect but do serve to give us further confidence in our system that we can identify genes specifically affecting satiety quiescence by locomotion and rule out genes that do not play a role. Most interestingly among signaling groups we have tested is endocannabinoid signaling. While this is a collaboration between our lab and Dr. Matthew Gill, who is investigating numerous aspects of the biology, we are very interested in how this affects satiety quiescence. Stimulation of the CB1 receptor increases appetite and food intake and so blocking the receptor should have the opposite effect. Treating worms with the mammalian CB1 receptor antagonist AM251 has a clear effect on behavior, increasing locomotion by increasing percent time roaming in both fasted and nonfasted animals. However, there is no known worm homolog of the mammalian CB1 receptor, so we cannot perform the proper control of using receptor knockout animals and demonstrating that we lose the effect. This also makes it very difficult to find whether endocannabinoid signaling

interacts with the cGMP-TGF β signaling axis and if so in what cell(s) without knowing the target of the antagonist. Identifying the target of AM251 in worms is currently being pursued by Dr. Gill's lab. Additionally, worms with NAE synthesis genes *nape-1* and *nape-2* overexpressed show some effects on satiety quiescence but we do not yet have worms with these genes knocked out, which is also currently being undertaken by the Gill lab. Altogether, this makes pursuing this line of research difficult to separate specific satiety quiescence signals from what might be a general avoidance response to a potentially noxious or harsh stimulus.

A few experiments that could begin to outline the interactions between these two signaling groups would be to test worms with enhanced and suppressed quiescence, *egl-4(gf)* and *egl-4(lf)* respectively, both fasted-refed and nonfasted with the inhibitor. If AM251 does not further enhance roaming in *egl-4(lf)* worms and does not suppress quiescence in *egl-4(gf)* worms, then NAE signaling could potentially be placed upstream of *egl-4*. If this is the case, it is a very good starting point because Dr. Gill's lab is investigating NAE signaling interacting with the *daf-2* pathway, which is upstream of *egl-4*. If this is not the case, if *egl-4(lf)* worms show increased roaming and *egl-4(gf)* worms show decreased quiescence it could mean that endocannabinoid signaling is acting parallel or downstream of *egl-4* affecting locomotion or that some quality of the drug is having a general aversive response. This could be answered by exogenous treatment of NAEs, which should have the opposite effect.

All together, we have developed a highly quantitative system to assay worm behavioral state over extended periods of time. We have used this system to further

investigate satiety quiescence signaling, finding additional components and interactions of the cGMP-TGF β signaling axis as well as begin to investigate other candidate pathways. We have established the ASI neuron as a major center of integration of nutritional information, finding an additional level of regulation of TGF β by cGMP as well as showing EGL-4 conveying satiety signaling in the neuron. Further, we have shown that ASI directly responds to the nutritional content of the worm's environment by activating in response to food. We then found that the TGF β ligand synthesized in ASI acts by binding its receptor on the RIM and RIC interneurons to convey satiety signaling. The work presented here and the work that is currently ongoing helps us to better understand the evolutionarily conserved genetic signaling that governs appetite control.

4. Materials and Methods

Strains and culture conditions

Worms were cultured and handled as described previously (112) with the following modifications: worms were routinely grown on NGMSR plates (105). All worms were maintained at 20 °C on *E. coli* strain HB101 unless indicated otherwise. The wild-type strain was *C. elegans* variant Bristol, strain N2. Mutant strains used were FK234 *egl-4(ks62)* IV, DA521 *egl-4(ad450sd)* IV, CB1372 *daf-7(e1372ts)* III, CB1393 *daf-8(e1393ts)* I, DR40 *daf-1(m40ts)* IV, KQ380 *daf-1(m40ts)* IV; *ftEx205[ptdc-1::daf-1-gfp odr-1::dsRed]*, DA2316 *daf-1(ad2316)* IV, DA2318 *daf-1(ad2316)* IV; *ftEx205[ptdc-1::daf-1-gfp odr-1::dsRed]*, DA2228 *adEx2228[gpa-4p::egl-4CA rol-6p::GFP]*, DA2225 *adEx2225[tax-4p::egl-4CA rol-6p::GFP]*, DA2233 *egl-4(ks62)* IV; *adEx2233[gpa-4p::egl-4 rol-6::GFP]*, DA2145 *egl-4(ks62)* IV; *adEx2145[tax-4::egl-4 rol-6::GFP]*, DA2221 *daf-11(sa195ts)* V; *adEx2221[gpa-4p::daf-11 rol-6p::GFP]*, DA2258 *daf-7(e1372ts)* III; *adEx2258[tax-4p::egl-4gf rol-6p::GFP]*, DA2258 *daf-7(e1372ts)* III; *adEx2258[tax-4p::egl-4gf rol-6p::GFP]*, DA2313 *tdc-1(ok914)* II; *daf-7(e1372ts)* III, DR47 *daf-11(m47)* V, DA2318 *daf-1(ad2316)* IV; *ftEx205[ptdc-1::daf-1-gfp odr-1::dsRED]*, DA2230 *adEx2230[gpa-4p::egl-4(gf) rol-6p::GFP]* KQ280 *daf-1(m40ts)* IV; *ftEx98[pdaf-1::daf-1-gfp odr-1::dsRED]*, KQ324 *daf-1(m40ts)* IV; *ftEx175[pB0280.7::daf-1-gfp odr-1::dsRED]*, KQ275 *daf-1(m40ts)* IV; *ftEx93[pglr-1::daf-1-gfp odr-1::dsRED]*, KQ251 *daf-1(m40ts)* IV; *ftEx69[pegl-3::daf-1-gfp odr-1::dsRED]*, KQ265 *daf-1(m40ts)* IV; *ftEx83[posm-6::daf-1-gfp odr-1::dsRED]*, KQ315 *daf-1(m40ts)*

IV; ftEx166[pflp-1::daf-1-gfp odr-1::dsRED], KQ380 *daf-1(m40ts) IV; ftEx205[ptdc-1::daf-1-gfp odr-1::dsRED]*, KQ332 *daf-1(m40ts) IV; ftEx183[pglr-7::daf-1-gfp odr-1::dsRED]*, PY7505 (Beverly et al., 2011), DA2227 *adEx2227[gpa-4p::GFP]*,

Locomotion analysis

5 ml LB was inoculated with a single colony of *E. coli* strain HB101 expressing mCherry and incubated shaking overnight at 37 °C. The culture was removed from the incubator and allowed to sit at room temperature overnight. The sample was centrifuged at 4,000 RPM for 3 minutes. After decanting the supernatant, the pellet was resuspended in the small residual amount of broth and transferred to a microcentrifuge tube. 40 µl of this suspension was twice serially diluted 1:1 with M9 (for a final 4× dilution). 5 µL of this suspension was pipetted onto a 35 mm NGMSR plate and allowed to dry completely.

Aztreonam was used to prepare low-quality food (39). Aztreonam prevents bacterial cell division, so that the bacteria turn into long snakes, which are difficult for the worm to swallow. Aztreonam-treated bacteria were prepared as above with one additional step. After shaking overnight at 37 °C, 1 ml of turbid LB was added to 4 ml fresh LB and aztreonam (Sigma-Aldrich) was added to a final concentration of 5 µg/ml. This was incubated overnight shaking at 37 °C, and then allowed to sit at room temperature overnight. For assays with aztreonam not incubated, bacteria were prepared the same as non-treated bacteria except for aztreonam being added to a final concentration of 5 µg/ml immediately before being centrifuged.

L4 worms were picked to a fresh NGMSR plate and given 8 hours to develop to young adult stage. Young adult worms (adults containing no eggs) were picked to individual 60 mm NGMSR plates without food and starved for 12-14 hours. A single starved worm was then transferred to an approximately 6 mm diameter spot of bacteria made by placing 5 μ l bacterial culture on a plate, focused under the camera, and allowed to refeed for 3 hours. The microscope light was then turned on and video capture was started at 1 frame/second for 1 hour.

For non-fasted assays, worms were prepared identically except that young adults were transferred to a 60 mm NGMSR plate with food for 12-14 hours and worms were given 30 minutes on the assay plate to recover from being transferred, followed by taking a 30 minute video at 1 frame/second.

Initial worm recordings were performed using a Leica MZ6 microscope at 2.5 \times magnification with a 1.0 \times lens and a Retiga-4000R camera and Image Pro Plus 6.2. Locomotion videos were analyzed by Image Pro Plus software. Subsequent analyses using TOBO were recorded using Point Grey GRAS-14S5M-C digital cameras fitted with a Computar MLM3X-MP macro zoom lenses. Images were recorded using Point Grey's freely available FlyCap2 software and worms were tracked using custom written program in MATLAB. A low pass filter was applied to each frame of the movie and the light/dark threshold was adjusted to find the outline of the worm. The center of mass was calculated at each time, reducing each recording to a series of (t, x, y) points, which were the basis for all subsequent analyses.

A certain amount of motion is detected even from a completely stationary worm, as small fluctuations in measured brightness of border pixels cause them to vary above and below threshold. This noise motion places a limit on our ability to detect immobility and therefore quiescence. To quantify it, we recorded a worm immobilized with 30 μl of 1M sodium azide before transfer to the assay plate. The mean measured speed of an immobilized worm was $0.32 \mu\text{m s}^{-1}$, and the speed was below $1 \mu\text{m s}^{-1}$ 99.7% of the time. Apparent motion was biased along one direction, as expected, since most border pixels are farther from the center in the anterior/posterior direction than in the dorsal/ventral direction.

Unbiased closed-loop fits

Given guesses of the behavioral states, an HMM fit can be performed on a track and new estimates calculated as described above (an *open-loop fit*, Figure 25A). Instead of stopping there, however, one can feed these new estimates into a second HMM fit of the same track to obtain a third set of estimates, and so on. Under favorable conditions the estimates will eventually stop changing. We call this a *closed-loop fit* (Figure 25B). Some adjustments were necessary to achieve convergence in closed-loop fits. First, we do not use re-estimated transition probabilities, but constrain them to the form described above. Second, we do not allow the variance parameters to vary independently for the separate states, but instead calculate a single value for each of these as a weighted average of the estimates for the separate states.

Figure 26

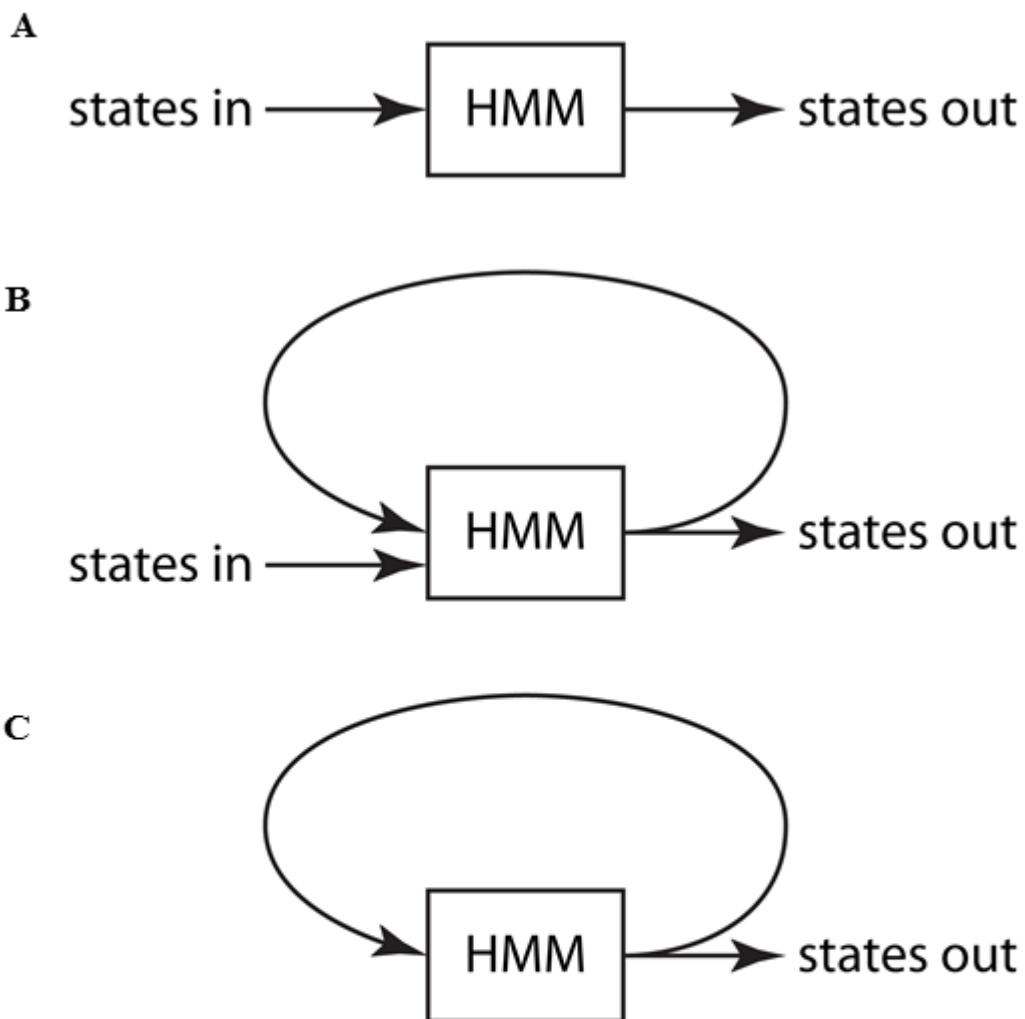


Figure 26. HMM fit scheme.

A. Open loop fit.

B. Closed loop fit.

C. Unbiased closed loop fit.

Because of the form of the distribution we assumed, this ensured that the ratios of emission probabilities were bounded. After convergence, we run the states through a single round of open-loop fit with these constraints relaxed so as to estimate transition probabilities and independent variance parameters for each state. We also did a single step of the Baum-Welch algorithm (113) for estimating the symbol probability matrix for an HMM with discrete emissions.

The closed-loop fit still requires initial guesses of state parameters to get started, and it is conceivable that these initial guesses might influence the states eventually discovered. In an *unbiased closed-loop fit*, initial guesses derived entirely from the data (Figure 25C). We began by fitting the data to a one-state model. In this case no initial guess is necessary, since the worm must be in the single state with probability 1 during the entire track. We then split the state into two, one identical to that derived from the one-state fit, and a second with slightly greater mean speed, and used these as the initial estimates for a two-state closed-loop fit. Although the fit began with two almost identical states, the slightly higher-speed state has higher probability during portions of the track when the worm is moving faster and the lower-speed state when the worm is moving slower. If there are coherent behavioral variations, the low and high-speed states will therefore take on different characteristics on parameter re-estimation, and during subsequent iterations they converge on different parts of the track. If the two-state fit converged, its higher-speed state was split in the same way to produce initial guesses for a three-state fit. Goodness of fit, measured by likelihood, tended to increase with more states: log-likelihood per point increased by 0.34 ± 0.20 (mean \pm standard deviation; range

0.013 – 1.14, $p < 10^{-60}$, signed rank test) in going from one to two states, and 0.069 ± 0.065 (range -0.016 – 0.35, $p < 10^{-59}$). (In 18/363 cases likelihood decreased slightly in going from two to three states. It is not surprising that likelihood decreased slightly in some cases, since the unbiased parameter estimates (34,114), are not maximum likelihood estimates. The equal variance constraint can also prevent achieving maximum likelihood.) We didn't try to continue past three states, since in most three-state fits there was at least one in which the worm spent little time. The fit with the highest excess entropy was used for further analysis.

Although we refer to these fits an “unbiased”, we recognize that this description is relative. Any method of recognizing behavioral patterns will of course be biased by the data collected. More subtly, to use the method it is necessary to reduce possible patterns of behavior to numerical descriptions, as described above. There is no fixed recipe for developing such a description scheme, and it determines what sort of patterns can be recognized.

Standard state descriptions and fits

While unbiased closed-loop fits capture a lot of information about an individual worm's movement, they are difficult to compare to published results. We therefore developed standard roaming, dwelling, and quiescence state descriptions that could be used for fitting all tracks. While these standard state fits probably do not classify behavior as

accurately as unbiased fits, they have the advantage of describing behavior in familiar terms.

Based on past results, we identified *pure plays*—conditions under which a worm spends most of its time in one of the three states. These conditions were:

Roaming: well-fed wild-type worms on poor food, well-fed *egl-4* loss-of-function mutant worms on poor and medium-quality food. Poor food is *E coli* HB101 grown on aztreonam (39). Medium-quality is a mixture of aztreonam-treated and untreated. Poor food suppresses dwelling and quiescence, and *egl-4* is necessary for both (20,29,38).

Dwelling: well-fed *ttx-3*, *tax-4*, and *daf-7* loss-of-function mutant worms on good food (*E coli* HB101); *daf-7* loss-of-function mutant worms fasted for 12 hours, then refed for 3 hours on good food. Under our recording conditions well-fed worms show little quiescence on good food. *ttx-3* and *tax-4* are necessary for normal levels of roaming (29,39). *daf-7* worms have been reported to be defective in both roaming (39) and quiescence (20).

Quiescence: *egl-4* gain-of-function mutant worms fasted for 12 hours, then refed for 3 hours on good food (20,42).

Unfortunately, none of these is a perfect pure play. We therefore chose the most probable state from the unbiased closed-loop fit of each track as the basis for pure-play state descriptions. Two kinds of effects can be detected in standard state fits. First, a

treatment or genotype may affect the rate at which a worm switches between roaming, dwelling, and quiescence. Second, the treatment may affect the way a worm behaves when in a particular state. For instance, it has been suggested, and we confirmed, that roaming worms move faster on low-quality food (39)—this effect is in addition to the increase in the frequency of roaming. Interpretation of these fits is complicated by the fact that one effect can masquerade as the other. For instance, if in some genotypes dwelling worms behave in ways that are closer to quiescent worms, this may appear as an increase in the frequency of quiescence.

Statistically typical tracks

The short illustrative statistically typical segments in Figure 3 in were chosen as follows. First, the most probable states from unbiased closed-loop fits on which the corresponding standard state description was based (see above) were averaged to get the target state. Next, the state descriptions were standardized to have standard deviation 1, and that state and track that yielded a standardized description closest to the mean were chosen. Finally, the central 90 s from the longest segment within this track in which the probability of being in this state remained continuously at $\geq 99\%$ was chosen.

A complete description of the calculations and parameters of the HMM is available in our paper ‘The Geometry of Locomotive Behavioral States in *C. elegans*’ Gallagher et al. (2013) (45).

Software

MATLAB and Mathematica scripts developed for this analysis are available at <http://elegans.som.vcu.edu/~leon/HMM>.

Food Intake Assay

Food intake were measured as previously described (20). Briefly, for the ‘fasted and refed’ test, worms were fasted for 12 hours and refed for 3 or 6 hours to examine satiety quiescence. Once worms were found to be quiescent, the duration was measured for 10 worms then averaged. To measure food intake, mCherry-expressing *E. coli* strain HB101 was inoculated in LB and grown overnight at 37 °C, then seeded on 35 mm NGMSR agar plates and incubated overnight at 37 °C. Plates were stored at room temperature for at least one night. Worms were fasted and refed as described (20). After 3 hours of refeeding, worms were treated with 100 µl of 1 M sodium azide for their feeding status to be fixed. Worms were observed using a Zeiss Axio A2 Imager with a 10× objective lens. Images were acquired using Zeiss Axiovision software and fluorescence was quantified using ImageJ.

Calcium Imaging

All calcium imaging experiments were performed on an Olympus BX51 upright microscope with a long-working-distance 40× water immersion objective and a Photometrics Evolve 128 EM-CCD camera. Analysis of the imaging data was performed

with a custom Java-based program as in Suzuki et al. (115), with one region of interest placed on ASI and a second placed nearby to measure background.

Young adult worms expressing the transgene were picked and placed in a microfluidic device that restrains the worm with the tip of the head (where the ASI sensory neurons are located) in a stream that can be rapidly switched ((99), "the olfactory chip"). Images were recorded at 100 frames/second for 60 seconds. Each worm was recorded for a 15 second baseline, followed by exposure to stimulus for 15 seconds, 15 seconds no stimulus, and a second 15 second exposure to stimulus.

DAF-7 Quantification

Worms expressing *daf-7p::daf-7::mCherry* were prepared the same as for fasted-refed assays. HB101 was inoculated in LB and grown overnight at 37 °C, then seeded on 35 mm NGMSR agar plates and incubated overnight at 37 °C. Plates were stored at room temperature for at least one night. Worms were either fasted and refed or nonfasted as described above. For cGMP treatment, 8-Br-cGMP was added to plates to a final concentration of 1 mM and worms were placed on the plate with no food. After 3 hours of refeeding or cGMP treatment or 30 minutes of mock refeeding, worms were treated with 100 µl of 1 M sodium azide for their feeding status to be fixed. Worms were observed using a Zeiss Axio A2 Imager with a 63X objective lens. Images were acquired using Zeiss Axiovision software and fluorescence was quantified using ImageJ.

Body Size Measurement

L4 stage worms were picked to a new plate on a lawn of HB101 bacteria. Worms were picked under fluorescence to sort transgenic and nontransgenic worms. The worms were grown at 20 °C for 24 hours (day one adults) or 48 hours (day two adults). To measure body size, worms were transferred to a plate with no bacteria and imaged using a Zeiss Discovery V8 microscope and a Point Grey RoHS 1.4MP B&W Grasshopper 1394b Camera at 7.5 frames/second. The area of each worm was calculated using a custom written MATLAB program. The area of the worm in seven consecutive frames was calculated and the result averaged.

Statistics

All bar graphs denote mean \pm SEM. Statistical tests were done using MatLab, Mathematica, and R programming tools.

Literature Cited

Literature Cited

1. Ogden CL, Carroll MD. Prevalence of Overweight, Obesity, and Extreme Obesity Among Adults: United States, Trends 1960–1962 Through 2007–2008. Natl Heal Nutr Exam Surv [Internet]. 2010; Available from:
http://www.cdc.gov/NCHS/data/hestat/obesity_adult_07_08/obesity_adult_07_08.pdf
2. Flegal KM CM. Prevalence and trends in obesity among us adults, 1999-2008. JAMA. 2010 Jan 20;303(3):235–41.
3. NHLBI Obesity Education Initiative Expert Panel on the Identification, Evaluation, and Treatment of Obesity in Adults (US). Clinical Guidelines on the Identification, Evaluation, and Treatment of Overweight and Obesity in Adults: The Evidence Report. Bethesda (MD): National Heart, Lung, and Blood Institute; 1998 Sep. Available from:
<http://www.ncbi.nlm.nih.gov/books/NBK2003/>.
4. O’Rahilly S, Farooqi IS, Yeo GSH, Challis BG. Minireview: Human Obesity—Lessons from Monogenic Disorders. Endocrinology. 2003 Sep 1;144(9):3757–64.
5. Friedman JM. A War on Obesity, Not the Obese. Science. 2003 Feb 7;299(5608):856–8.

6. Comuzzie AG, Allison DB. The Search for Human Obesity Genes. *Science*. 1998 May 29;280(5368):1374–7.
7. Chen H, Charlat O, Tartaglia LA, Woolf EA, Weng X, Ellis SJ, et al. Evidence That the Diabetes Gene Encodes the Leptin Receptor: Identification of a Mutation in the Leptin Receptor Gene in db/db Mice. *Cell*. 1996 Feb 9;84(3):491–5.
8. Zhang Y, Proenca R, Maffei M, Barone M, Leopold L, Friedman JM. Positional cloning of the mouse obese gene and its human homologue. *Nature*. 1994 Dec 1;372(6505):425–32.
9. Mutch DM, Clément K. Unraveling the Genetics of Human Obesity. *PLoS Genet*. 2006 Dec 29;2(12):e188.
10. Christopher G. Bell, Andrew J. Walley, Philippe Froguel. The genetics of human obesity. *Nat Rev Genet*. 2005;6(3):221–34.
11. Chambers AP, Sandoval DA, Seeley RJ. Integration of Satiety Signals by the Central Nervous System. *Curr Biol CB*. 2013 May 6;23(9):R379–R388.
12. Schwartz MW, Woods SC, Porte D, Seeley RJ, Baskin DG. Central nervous system control of food intake. *Nature*. 2000 Apr 6;404(6778):661–71.
13. Antin J, Gibbs J, Holt J, Young RC, Smith GP. Cholecystokinin elicits the complete behavioral sequence of satiety in rats. *J Comp Physiol Psychol*. 1975 Sep;89(7):784–90.

14. Ishii Y, Blundell JE, Halford JCG, Rodgers RJ. Palatability, food intake and the behavioural satiety sequence in male rats. *Physiol Behav.* 2003;80(1):37 – 47.
15. Halford JCG, Wanninayake SCD, Blundell JE. Behavioral Satiety Sequence (BSS) for the Diagnosis of Drug Action on Food Intake. *Pharmacol Biochem Behav.* 1998;61(2):159 – 168.
16. Spudeit WA, Sulzbach NS, Bittencourt M de A, Duarte AMC, Liang H, Lino-de-Oliveira C, et al. The behavioral satiety sequence in pigeons (*Columba livia*). Description and development of a method for quantitative analysis. *Physiol Behav.* 2013;122(0):62 – 71.
17. Wren AM, Bloom SR. Gut Hormones and Appetite Control. *Gastroenterology.* 2007;132(6):2116 – 2130.
18. Hetherington AW, Ranson SW. Hypothalamic lesions and adiposity in the rat. *Anat Rec.* 1940;78(2):149–72.
19. Elmquist JK, Elias CF, Saper CB. From lesions to leptin: hypothalamic control of food intake and body weight. *Neuron.* 1999 Feb;22(2):221–32.
20. You Y, Kim J, Raizen DM, Avery L. Insulin, cGMP, and TGF-beta signals regulate food intake and quiescence in *C. elegans*: a model for satiety. *Cell Metab.* 2008 Mar;7(3):249–57.

21. Johnen H, Lin S, Kuffner T, Brown DA, Tsai VW-W, Bauskin AR, et al. Tumor-induced anorexia and weight loss are mediated by the TGF- β superfamily cytokine MIC-1. *Nat Med*. 2007 Nov;13(11):1333–40.
22. Arora S, Anubhuti. Role of neuropeptides in appetite regulation and obesity – A review. *Neuropeptides*. 2006;40(6):375 – 401.
23. Valentino MA, Lin JE, Snook AE, Li P, Kim GW, Marszalowicz G, et al. A uroguanylin-GUCY2C endocrine axis regulates feeding in mice. *J Clin Invest*. 2011 Sep 1;121(9):3578–88.
24. Jones KT, Ashrafi K. *Caenorhabditis elegans* as an emerging model for studying the basic biology of obesity. *Dis Model Mech*. 2009 May 1;2(5-6):224–9.
25. Kahn BB, Alquier T, Carling D, Hardie DG. AMP-activated protein kinase: Ancient energy gauge provides clues to modern understanding of metabolism. *Cell Metab*. 2005;1(1):15 – 25.
26. Watts JL. Fat synthesis and adiposity regulation in *Caenorhabditis elegans*. *Trends Endocrinol Metab*. 2009 Mar 1;20(2):58–65.
27. Zheng J, Greenway FL. *Caenorhabditis elegans* as a model for obesity research. *Int J Obes*. 2012 Feb;36(2):186–94.

28. Ashrafi, K. Obesity and the regulation of fat metabolism (March 9, 2007), WormBook, ed. The C. elegans Research Community, WormBook, doi/10.1895/wormbook.1.130.1, <http://www.wormbook.org>.
29. Shtonda BB, Avery L. Dietary choice behavior in *Caenorhabditis elegans*. *J Exp Biol*. 2006 Jan 1;209(1):89–102.
30. Williams KW, Elmquist JK. From neuroanatomy to behavior: central integration of peripheral signals regulating feeding behavior. *Nat Neurosci*. 2012 Oct;15(10):1350–5.
31. Avery L, Shtonda BB. Food transport in the *C. elegans* pharynx. *J Exp Biol*. 2003 Jul 15;206(14):2441–57.
32. Hart, Anne C., ed. Behavior (July 3, 2006), WormBook, ed. The C. elegans Research Community, WormBook, doi/10.1895/wormbook.1.87.1, <http://www.wormbook.org>.
33. Avery L, Horvitz HR. Effects of starvation and neuroactive drugs on feeding in *Caenorhabditis elegans*. *J Exp Zool*. 1990;253(3):263–70.
34. Sawin ER, Ranganathan R, Horvitz HR. *C. elegans* Locomotory Rate Is Modulated by the Environment through a Dopaminergic Pathway and by Experience through a Serotonergic Pathway. *Neuron*. 2000;26(3):619 – 631.
35. You Y, Kim J, Cobb M, Avery L. Starvation activates MAP kinase through the muscarinic acetylcholine pathway in *Caenorhabditis elegans* pharynx. *Cell Metab*. 2006 Apr 1;3(4):237–45.

36. Avery, L. and You, Y.J. C. elegans feeding (May 21, 2012), WormBook, ed. The C. elegans Research Community, WormBook, doi/10.1895/wormbook.1.150.1, <http://www.wormbook.org>.
37. You Y-J, Avery L. Appetite control: worm's-eye-view. *Anim Cells Syst*. 2012 Aug 31;16(5):351–6.
38. Fujiwara M, Sengupta P, McIntire SL. Regulation of Body Size and Behavioral State of C. elegans by Sensory Perception and the EGL-4 cGMP-Dependent Protein Kinase. *Neuron*. 2002 Dec 19;36(6):1091–102.
39. Ben Arous J, Laffont S, Chatenay D. Molecular and Sensory Basis of a Food Related Two-State Behavior in C. elegans. *PLoS ONE*. 2009 Oct 23;4(10):e7584.
40. Hills T, Brockie PJ, Maricq AV. Dopamine and Glutamate Control Area-Restricted Search Behavior in Caenorhabditis elegans. *J Neurosci*. 2004 Feb 4;24(5):1217–25.
41. Van Buskirk C, Sternberg, PW. Epidermal growth factor signaling induces behavioral quiescence in Caenorhabditis elegans. *Nat Neurosci*. 2007;10(10):1300–7.
42. Raizen DM, Zimmerman JE, Maycock MH, Ta UD, You Y, Sundaram MV, et al. Lethargus is a Caenorhabditis elegans sleep-like state. *Nature*. 2008;451(7178):569–72.
43. Avery L. Caenorhabditis elegans behavioral genetics: where are the knobs? *BMC Biol*. 2010;8(1):69.

44. Hao Y, Xu N, Box AC, Schaefer L, Kannan K, Zhang Y, et al. Nuclear cGMP-Dependent Kinase Regulates Gene Expression via Activity-Dependent Recruitment of a Conserved Histone Deacetylase Complex. *PLoS Genet.* 2011;7(5):e1002065.
45. Gallagher T, Bjorness T, Greene R, You Y-J, Avery L. The Geometry of Locomotive Behavioral States in *C. elegans*. *PLoS ONE.* 2013 Mar 28;8(3):e59865.
46. Gallagher T, Kim J, Oldenbroek M, Kerr R, You Y-J. ASI Regulates Satiety Quiescence in *C. elegans*. *J Neurosci.* 2013 Jun 5;33(23):9716–24.
47. Flavell SW, Pokala N, Macosko EZ, Albrecht DR, Larsch J, Bargmann CI. Serotonin and the Neuropeptide PDF Initiate and Extend Opposing Behavioral States in *C. elegans*. *Cell.* 2013 Aug 29;154(5):1023–35.
48. Trent C, Tsung N, Horvitz HR. EGG-LAYING DEFECTIVE MUTANTS OF THE NEMATODE CAENORHABDITIS ELEGANS. *Genetics.* 1983 Aug 1;104(4):619–47.
49. Hirose T, Nakano Y, Nagamatsu Y, Misumi T, Ohta H, Ohshima Y. Cyclic GMP-dependent protein kinase EGL-4 controls body size and lifespan in *C. elegans*. *Dev Camb Engl.* 2003 Mar;130(6):1089–99.
50. Ren P, Lim CS, Johnsen R, Albert PS, Pilgrim D, Riddle DL. Control of *C. elegans* larval development by neuronal expression of a TGF-beta homolog. *Science.* 1996 Nov 22;274(5291):1389–91.

51. Schackwitz WS, Inoue T, Thomas JH. Chemosensory Neurons Function in Parallel to Mediate a Pheromone Response in *C. elegans*. *Neuron*. 1996;17(4):719 – 728.
52. L'Etoile ND, Bargmann CI. Olfaction and Odor Discrimination Are Mediated by the *C. elegans* Guanylyl Cyclase ODR-1. *Neuron*. 2000;25(3):575 – 586.
53. Schaap P. Guanylyl cyclases across the tree of life. *Front Biosci*. 2005;10:1485–98.
54. Johnson J-LF, Leroux MR. cAMP and cGMP signaling: sensory systems with prokaryotic roots adopted by eukaryotic cilia. *Trends Cell Biol*. 2010;20(8):435 – 444.
55. Marden JN, Dong Q, Roychowdhury S, Berleman JE, Bauer CE. Cyclic GMP controls *Rhodospirillum centenum* cyst development. *Mol Microbiol*. 2011;79(3):600–15.
56. Ortiz CO, Etchberger JF, Posy SL, Frøkjær-Jensen C, Lockery S, Honig B, et al. Searching for Neuronal Left/Right Asymmetry: Genomewide Analysis of Nematode Receptor-Type Guanylyl Cyclases. *Genetics*. 2006 May 1;173(1):131–49.
57. Liu J, Ward A, Gao J, Dong Y, Nishio N, Inada H, et al. *C. elegans* phototransduction requires a G protein-dependent cGMP pathway and a taste receptor homolog. *Nat Neurosci*. 2010 Jun;13(6):715–22.
58. Inada H, Ito H, Satterlee J, Sengupta P, Matsumoto K, Mori I. Identification of Guanylyl Cyclases That Function in Thermosensory Neurons of *Caenorhabditis elegans*. *Genetics*. 2006 Apr 1;172(4):2239–52.

59. Gray JM, Karow DS, Lu H, Chang AJ, Chang JS, Ellis RE, et al. Oxygen sensation and social feeding mediated by a *C. elegans* guanylate cyclase homologue. *Nature*. 2004;430(6997):317–22.
60. Couto A, Oda S, Nikolaev VO, Soltesz Z, de Bono M. In vivo genetic dissection of O₂-evoked cGMP dynamics in a *Caenorhabditis elegans* gas sensor. *Proc Natl Acad Sci [Internet]*. 2013 Aug 12; Available from: <http://www.pnas.org/content/early/2013/08/08/1217428110.abstract>
61. Murayama T, Takayama J, Fujiwara M, Maruyama IN. Environmental Alkalinity Sensing Mediated by the Transmembrane Guanylyl Cyclase GCY-14 in *C. elegans*. *Curr Biol CB*. 2013 Jun 3;23(11):1007–12.
62. Coburn CM, Bargmann CI. A Putative Cyclic Nucleotide–Gated Channel Is Required for Sensory Development and Function in *C. elegans*. *Neuron*. 1996 Oct 1;17(4):695–706.
63. Komatsu H, Mori I, Rhee J-S, Akaike N, Ohshima Y. Mutations in a Cyclic Nucleotide–Gated Channel Lead to Abnormal Thermosensation and Chemosensation in *C. elegans*. *Neuron*. 1996 Oct;17(4):707–18.
64. Birnby DA, Link EM, Vowels JJ, Tian H, Colacurcio PL, Thomas JH. A Transmembrane Guanylyl Cyclase (DAF-11) and Hsp90 (DAF-21) Regulate a Common Set of Chemosensory Behaviors in *Caenorhabditis elegans*. *Genetics*. 2000 May 1;155(1):85–104.

65. Coates JC, de Bono M. Antagonistic pathways in neurons exposed to body fluid regulate social feeding in *Caenorhabditis elegans*. *Nature*. 2002 Oct 31;419(6910):925–9.
66. Daniels SA, Ailion M, Thomas JH, Sengupta P. *egl-4* Acts Through a Transforming Growth Factor- β /SMAD Pathway in *Caenorhabditis elegans* to Regulate Multiple Neuronal Circuits in Response to Sensory Cues. *Genetics*. 2000 Sep 1;156(1):123–41.
67. Raizen DM, Cullison KM, Pack AI, Sundaram MV. A Novel Gain-of-Function Mutant of the Cyclic GMP-Dependent Protein Kinase *egl-4* Affects Multiple Physiological Processes in *Caenorhabditis elegans*. *Genetics*. 2006 May 1;173(1):177–87.
68. Kaun KR, Sokolowski MB. cGMP-dependent protein kinase: linking foraging to energy homeostasis. *Genome*. 2008 Nov 26;52(1):1–7.
69. Osborne KA, Robichon A, Burgess E, Butland S, Shaw RA, Coulthard A, et al. Natural Behavior Polymorphism Due to a cGMP-Dependent Protein Kinase of *Drosophila*. *Science*. 1997 Aug 8;277(5327):834–6.
70. Kaun KR, Riedl CAL, Chakaborty-Chatterjee M, Belay AT, Douglas SJ, Gibbs AG, et al. Natural variation in food acquisition mediated via a *Drosophila* cGMP-dependent protein kinase. *J Exp Biol*. 2007 Oct 15;210(20):3547–58.
71. Breer H, Shepherd GM. Implications of the NO/cGMP system for olfaction. *Trends Neurosci*. 1993;16(1):5 – 9.

72. Rosenzweig S, Yan W, Dasso M, Spielman AI. Possible Novel Mechanism for Bitter Taste Mediated Through cGMP. *J Neurophysiol.* 1999 Apr 1;81(4):1661–5.
73. Krizhanovsky V, Agamy O, Naim M. Sucrose-stimulated subsecond transient increase in cGMP level in rat intact circumvallate taste bud cells. *Am J Physiol - Cell Physiol.* 2000;279(1):C120–C125.
74. Wang X, Robinson PJ. Cyclic GMP-Dependent Protein Kinase and Cellular Signaling in the Nervous System. *J Neurochem.* 1997;68(2):443–56.
75. Scheiner R, Sokolowski MB, Erber J. Activity of cGMP-Dependent Protein Kinase (PKG) Affects Sucrose Responsiveness and Habituation in *Drosophila melanogaster*. *Learn Mem.* 2004 May 1;11(3):303–11.
76. Dijke P ten, Hill CS. New insights into TGF- β -Smad signalling. *Trends Biochem Sci.* 2004;29(5):265 – 273.
77. Savage-Dunn, C. TGF- β signaling (September 9, 2005), WormBook, ed. The *C. elegans* Research Community, WormBook, doi/10.1895/wormbook.1.22.1, <http://www.wormbook.org>.
78. Riddle DL, Swanson MM, Albert PS. Interacting genes in nematode dauer larva formation. *Nature.* 1981 Apr 23;290(5808):668–71.

79. Golden JW, Riddle DL. A pheromone-induced developmental switch in *Caenorhabditis elegans*: Temperature-sensitive mutants reveal a wild-type temperature-dependent process. *Proc Natl Acad Sci U S A*. 1984 Feb;81(3):819–23.
80. Malone EA, Thomas JH. A screen for nonconditional dauer-constitutive mutations in *Caenorhabditis elegans*. *Genetics*. 1994 Mar 1;136(3):879–86.
81. Thomas JH, Birnby DA, Vowels JJ. Evidence for parallel processing of sensory information controlling dauer formation in *Caenorhabditis elegans*. *Genetics*. 1993 Aug 1;134(4):1105–17.
82. Hu PJ. Dauer. *WormBook: the online review of C elegans biology* <http://wormbook.org>. 2007.
83. Bargmann CI, Horvitz HR. Control of larval development by chemosensory neurons in *Caenorhabditis elegans*. *Science*. 1991 Mar 8;251(4998):1243–6.
84. Ailion M, Thomas JH. Dauer Formation Induced by High Temperatures in *Caenorhabditis elegans*. *Genetics*. 2000 Nov 1;156(3):1047–67.
85. Stansberry J, Baude EJ, Taylor MK, Chen P-J, Jin S-W, Ellis RE, et al. A cGMP-dependent protein kinase is implicated in wild-type motility in *C. elegans*. *J Neurochem*. 2001;76(4):1177–87.

86. Estevez M, Attisano L, Wrana JL, Albert PS, Massague J, Riddle DL. The *daf-4* gene encodes a bone morphogenetic protein receptor controlling *C. elegans* dauer larva development. *Nature*. 1993 Oct 14;365(6447):644–9.
87. Georgi LL, Albert PS, Riddle DL. *daf-1*, a *C. elegans* gene controlling dauer larva development, encodes a novel receptor protein kinase. *Cell*. 1990 May 18;61(4):635–45.
88. Gunther CV, Georgi LL, Riddle DL. A *Caenorhabditis elegans* type I TGF beta receptor can function in the absence of type II kinase to promote larval development. *Development*. 2000 Aug 1;127(15):3337–47.
89. Murakami M, Koga M, Ohshima Y. DAF-7/TGF-beta expression required for the normal larval development in *C. elegans* is controlled by a presumed guanylyl cyclase DAF-11. *Mech Dev*. 2001 Nov;109(1):27–35.
90. Gruninger TR, Gualberto DG, Garcia LR. Sensory Perception of Food and Insulin-Like Signals Influence Seizure Susceptibility. *PLoS Genet*. 2008;4(7):e1000117.
91. Shoval O, Sheftel H, Shinar G, Hart Y, Ramote O, Mayo A, et al. Evolutionary Trade-Offs, Pareto Optimality, and the Geometry of Phenotype Space. *Science*. 2012 Jun 1;336(6085):1157–60.
92. Chelur DS, Chalfie M. Targeted cell killing by reconstituted caspases. *Proc Natl Acad Sci*. 2007 Feb 13;104(7):2283–8.

93. Beverly M, Anbil S, Sengupta P. Degeneracy and Neuromodulation among Thermosensory Neurons Contribute to Robust Thermosensory Behaviors in *Caenorhabditis elegans*. *J Neurosci*. 2011 Aug 10;31(32):11718–27.
94. Greer ER, Pérez CL, Van Gilst MR, Lee BH, Ashrafi K. Neural and molecular dissection of a *C. elegans* sensory circuit that regulates fat and feeding. *Cell Metab*. 2008 Aug;8(2):118–31.
95. Horvitz H, Chalfie M, Trent C, Sulston J, Evans P. Serotonin and octopamine in the nematode *Caenorhabditis elegans*. *Science*. 1982 May 28;216(4549):1012–4.
96. Alkema MJ, Hunter-Ensor M, Ringstad N, Horvitz HR. Tyramine Functions Independently of Octopamine in the *Caenorhabditis elegans* Nervous System. *Neuron*. 2005 Apr 21;46(2):247–60.
97. Jansen G, Thijssen KL, Werner P, van derHorst M, Hazendonk E, Plasterk RHA. The complete family of genes encoding G proteins of *Caenorhabditis elegans*. *Nat Genet*. 1999 Apr;21(4):414–9.
98. Nakai J, Ohkura M, Imoto K. A high signal-to-noise Ca²⁺ probe composed of a single green fluorescent protein. *Nat Biotech*. 2001 Feb;19(2):137–41.
99. Chronis N, Zimmer M, Bargmann CI. Microfluidics for in vivo imaging of neuronal and behavioral activity in *Caenorhabditis elegans*. *Nat Methods*. 2007 Sep;4(9):727–31.

100. DiPatrizio NV, Astarita G, Schwartz G, Li X, Piomelli D. Endocannabinoid signal in the gut controls dietary fat intake. *Proc Natl Acad Sci [Internet]*. 2011 Jul 5; Available from: <http://www.pnas.org/content/early/2011/06/27/1104675108.abstract>
101. Storr MA, Sharkey KA. The endocannabinoid system and gut–brain signalling. *Curr Opin Pharmacol*. 2007;7(6):575 – 582.
102. Woods SC. The Endocannabinoid System: Mechanisms Behind Metabolic Homeostasis and Imbalance. *Am J Med*. 2007;120(2, Supplement 1):S9–17.
103. Escartín-Pérez RE, Cendejas-Trejo NM, Cruz-Martínez AM, González-Hernández B, Mancilla-Díaz JM, Florán-Garduño B. Role of cannabinoid {CB1} receptors on macronutrient selection and satiety in rats. *Physiol Behav*. 2009;96(4–5):646 – 650.
104. Lucanic M, Held JM, Vantipalli MC, Klang IM, Graham JB, Gibson BW, et al. N-acylethanolamine signalling mediates the effect of diet on lifespan in *Caenorhabditis elegans*. *Nature*. 2011 May 12;473(7346):226–9.
105. Avery L. The genetics of feeding in *Caenorhabditis elegans*. *Genetics*. 1993 Apr;133(4):897–917.
106. Kiyama Y, Miyahara K, Ohshima Y. Active uptake of artificial particles in the nematode *Caenorhabditis elegans*. *J Exp Biol*. 2012 Apr 1;215(7):1178–83.

107. McKay JP, Raizen DM, Gottschalk A, Schafer WR, Avery L. eat-2 and eat-18 Are Required for Nicotinic Neurotransmission in the *Caenorhabditis elegans* Pharynx. *Genetics*. 2004 Jan 1;166(1):161–9.
108. Currie E, King B, Lawrenson AL, Schroeder LK, Kershner AM, Hermann GJ. Role of the *Caenorhabditis elegans* Multidrug Resistance Gene, *mrp-4*, in Gut Granule Differentiation. *Genetics*. 2007 Nov 1;177(3):1569–82.
109. Zheng Y, Brockie PJ, Mellem JE, Madsen DM, Maricq AV. Neuronal Control of Locomotion in *C. elegans* Is Modified by a Dominant Mutation in the GLR-1 Ionotropic Glutamate Receptor. *Neuron*. 1999;24(2):347 – 361.
110. Ben-Shahar Y, Robichon A, Sokolowski MB, Robinson GE. Influence of Gene Action Across Different Time Scales on Behavior. *Science*. 2002 Apr 26;296(5568):741–4.
111. Kawli T, Tan M-W. Neuroendocrine signals modulate the innate immunity of *Caenorhabditis elegans* through insulin signaling. *Nat Immunol*. 2008 Dec;9(12):1415–24.
112. Sulston J, Hodgkin J. *Methods*. (Wood, W. B., ed). *The Nematode Caenorhabditis elegans*. Cold Spring Harbor, New York: Cold Spring Harbor Press.; 1988. p. pp 587–606.

113. Press WH (2007) Numerical recipes : the art of scientific computing. Cambridge, UK; New York: Cambridge University Press. xxi, 1235 p.
114. Chen S, Lee AY, Bowens NM, Huber R, Kravitz EA. Fighting fruit flies: A model system for the study of aggression. Proc Natl Acad Sci. 2002 Apr 16;99(8):5664–8.
115. Suzuki H, Kerr R, Bianchi L, Frøkjær-Jensen C, Slone D, Xue J, et al. In Vivo Imaging of *C. elegans* Mechanosensory Neurons Demonstrates a Specific Role for the MEC-4 Channel in the Process of Gentle Touch Sensation. Neuron. 2003 Sep 11;39(6):1005–17.

VITA

Thomas Gallagher grew up in Scottsville, New York with his parents Mark and Linda Gallagher and younger siblings Terry and Erin. Tom graduated from Wheatland-Chili Jr/Sr Highschool in 2004 and attended the State University of New York College at Geneseo, graduating in 2008 with a Bachelors of Science in Biochemistry and a Minor in Mathematics. In the Fall of 2008 he enrolled in the PhD program in the Department of Biochemistry at Virginia Commonwealth University and eventually joined the lab of Dr. Young-Jai You in September 2010.